Global historical soybean and wheat yield loss estimates from ozone pollution considering water and temperature as modifying effects

Authors

Bernhard Schauberger[1,2*], Susanne Rolinski[1], Sibyll Schaphoff[1], Christoph Müller[1]

* Corresponding author: schauber@pik-potsdam.de, +33 1 69 08 77 24

[1] Potsdam Institute for Climate Impact Research (PIK), Telegrafenberg A31, 14473 Potsdam, Germany

[2] Laboratoire des Sciences du Climat et de l'Environnement, Institut Pierre-Simon Laplace (IPSL), 91191 Gif sur Yvette, France

Abstract

Ozone pollution can severely diminish crop yields. Its damaging effects depend, apart from ozone concentration, on crop, cultivar, water status, temperature and CO_2 concentration. Previous studies estimating global yield loss from ozone pollution did not consider all of these co-factors and climate change impact studies on crop yields typically ignore ozone pollution. Here we introduce an ozone damage module for the widely used process-based crop model LPJmL. The implementation describes ozone uptake through stomata, internal detoxification and short- and long-term effects on productivity and phenology, dynamically accounting for all listed co-factors. Using this enhanced model we estimate historical global yield losses from ozone pollution for wheat and soybeans. We divide wheat into "Western" and "Asian" to account for higher ozone sensitivities in Asian types. We apply daily ozone concentrations obtained from six chemistry-transport models provided by the ACCMIP and HTAP2 projects. Our implementation of ozone damage follows expected dynamics, for example damage amplification under irrigation. The model is able to reproduce results from chamber and field

studies. Historical ozone-induced losses between 2008 and 2010 vary between countries, and we estimate these between 2 and 10% of ozone-free yields for soybeans, between 0 and 27% for Western wheat and 4 and 39% for Asian wheat.

Our study highlights the threat of ozone pollution for global crop production and improves over previous studies by considering co-factors of ozone damage. Uncertainties of our study include the extrapolation from rather few point observations to the globe, possible biases in ozone data, omission of sub-daily fluctuations in ozone concentration or stomatal conductance and the averaging of different cultivars across regions. We suggest performing further field-scale experimental studies of ozone effects on crops, as these are currently rare but would be particularly helpful to evaluate models and to estimate large-scale effects of ozone.

Keywords: ozone, wheat, soybean, crop model, global, yield

Highlights

- Global yield damages from surface ozone are calculated for wheat and soybeans
- Air temperature and plant water status are considered as co-factors
- Ozone damage depends on region and cultivar, ranging from 0-39 % of harvest loss
- For wheat, Asia suffers from much higher losses than Europe or North America

1. Introduction

High levels of surface ozone (O_3) can lower crop yields substantially (Burney and Ramanathan, 2014; Fuhrer, 2009; Ghude et al., 2014; Long et al., 2005; McGrath et al., 2015; Mills et al., 2015). Up to date, pollutants including ozone may even have contributed more to yield changes than climate change (Shindell, 2016). Ozone is a powerful oxidant and the mechanisms how it affects plants have long been researched (Ainsworth et al., 2012; Wilkinson and Davies, 2010; Wilkinson et al., 2012). The gas enters plant leaves via the stomata and swiftly reacts with apoplast components to form reactive oxygen species (ROS). These react further with membranes and cell components and cause damages to enzymes, including photosynthesis proteins. This leads to lower rates of carbon (C) assimilation. To prevent damage, plants tend to lower stomatal conductance in the presence of O_3, causing reduced influx of CO_2 and thus also lower photosynthesis rates. Senescence is advanced with higher O_3 due to accumulating damages, causing a precocious loss of green leaf area. A share of assimilated carbon is respired for repairing ozone-induced damages and to build up anti-oxidant defenses like ascorbate. Additionally, ovary sterility or kernel abortion could ensue from ozone damage, leaving less sink capacity for yield formation. Furthermore, the weather conditions favorable for O_3 formation (dry, sunny and warm) may cause stress for plants, while their capacity to cope with stress is diminished due to O_3 (Wilkinson et al., 2012). All these effects lead to a lower net assimilation of C on short and long term, eventually resulting in lower yield levels. Wheat and soybean are two global staple crops (FAO, 2016) and deemed sensitive to O_3, with possibly increased damage potential of ozone in recent years due to higher stomatal conductance (Feng et al., 2008; McGrath et al., 2015; Osborne et al., 2016; Wilkinson et al., 2012). Ozone is also a greenhouse gas accelerating climate change and thus affecting yields indirectly (Fishman et al., 1979; IPCC, 2013; Sitch et al., 2007).

Ozone formation in the atmosphere is complex (Rai and Agrawal, 2012), largely determined by three limiting factors: solar radiation, temperature and precursor amount and relative proportion (methane, carbon monoxide, Volatile Organic Compounds (VOCs) and NO_x compounds). These factors can vary independently (Fuhrer, 2009; McGrath et al., 2015), leading to substantial variance in O_3 levels over space and time (Lin et al., 2015; Stevenson et al., 2006). Trends of ozone concentration diverge between regions. While in industrialized countries concentrations increased previously but have stabilized or slightly declined due to stricter enforcement of thresholds, O_3 trends are upwards in transition economies like India and China (Gaudel et al., 2018; Rao et al., 2016; The Royal Society, 2008). Quantifying the global impact of O_3 on crop yields is thus a pertinent issue.

There are numerous chamber and field studies quantifying the effect of increased O_3 on yields, reviewed, for example, by Broberg et al. (2015), Feng et al. (2008), Long et al. (2005), Morgan et al. (2003) or Rai and Agrawal (2012). Modeling studies based on experiments can be divided into three categories: exposure-response functions (ERF) for empirical correlations between yield and ozone exposure, flux-based approaches accounting for ozone uptake instead of exposure, and process-based models simulating physiological effects of O_3 on different plant processes. ERF's are readily computed for large geographical areas and produce reliable results under similar conditions as they were trained on (Musselman et al., 2006; Pleijel et al., 2007). Examples of ERF applications comprise Avnery et al. (2011) or Van Dingenen et al. (2009) where the authors calculate ozone damages for soybean, wheat and other crops in 2000, estimating losses between 4 and 16% depending on crop and region. Chuwah et al. (2015) study effects on eleven crops between 2005 and 2050 and derive that at least 2.5% of additional cropland area would be required to compensate for O_3-induced

production losses. Avnery et al. (2013) research two pathways to reduce crop damage: climate change mitigation or crop adaptation. Burney and Ramanathan (2014) apply damage functions to estimate wheat and rice loss in India, correlating yield with O_3 precursors rather than O_3 concentrations directly. Tai et al. (2014) study interactive effects between O_3 and temperature changes in 2000 and 2050 for four crops and assess the impact on food security. But these ERF-based assessments are agnostic about the underlying mechanisms how O_3 reduces yields. Additionally, interactions between O_3 and other environmental factors like CO_2 or water stress are usually not considered. Approaches that account for actual fluxes to the leaves, rather than outside concentrations, are thus necessary to complement experimental studies (Ainsworth et al., 2012; Franz et al., 2017). These could support adaptation or plant breeding for more O_3-resistant cultivars.

A hybrid between process-based and empirical models is the DO_3SE flux-based model by Emberson et al. (2000). Stomatal conductance is described in dependence of limiting factors including water stress, light, temperature and ozone. The resulting stomatal ozone flux can be distinct from ozone concentrations. The DO_3SE model has recently been applied in a novel combination of two model types: first, ozone flux to plants is calculated considering temperature, vapor pressure deficit, radiation and soil moisture, and, second, the ensuing damage to yields is then derived by a linear equation with this flux as exogenous variable (Mills et al., 2018a; Mills et al., 2018b). Another semi-empirical damage function is derived by Reilly et al. (2007) who calculate economic effects of interacting CO_2, O_3 and climate change on crop yields. But they only consider a generic C_3 crop on monthly time step.

Few process-based crop models including ozone stress have been designed. Fuhrer (2009) developed a model for O_3 damage with explicit stomatal conductance and detoxification, but remained on a conceptual basis. Sitch et al. (2007) assessed indirect effects of O_3 on climate change, but considered only generic vegetation and crops. Finally, Ewert and Porter (2000)

provide a detailed study of CO_2 and O_3 interactive effects on wheat yields. They consider short-term (reduced photosynthesis) and long-term (advanced senescence) damages of O_3, but do not include water stress effects or possible costs of cell repair measures. Emberson et al. (2018) provide an excellent overview of current modelling efforts and sketch next steps in capturing ozone effects on crops (see Discussion for details on how this study follows their recommendations).

In this study, we extend the global vegetation and crop model LPJmL (Bondeau et al., 2007; Schaphoff et al., 2018) towards ozone effects on crops. We model the effect of historical O_3 concentrations on global wheat and soybean yields. We explicitly consider interaction effects of O_3 with temperature, water stress, phenology and CO_2 at the physiological level in plants. We separately analyze Western (i.e. European and North American) and Asian wheat varieties to account for differences in their ozone responses (Emberson et al., 2009; Feng et al., 2012). This is, to our knowledge, the first study analyzing ozone-induced yield losses at the global scale with an integral consideration of modulating co-factors within a crop model.

2. Materials and methods

2.1 Crop model and crops

LPJmL is a widely used, process-based dynamic vegetation and crop model (Bondeau et al., 2007; Sitch et al., 2003; Waha et al., 2012). LPJmL simulates carbon (C) cycling and vegetation dynamics with explicit representation of physiological processes. These include photosynthesis, autotrophic respiration, transpiration, evaporation, interception and runoff in natural and agricultural systems. The model is driven by daily weather (temperature, precipitation, incoming shortwave radiation and net downward longwave radiation), atmospheric CO_2 concentrations and soil texture. Agriculture is described by managed grasslands and twelve crop functional types that differ in bio-climatic limits and eco-physiological parameters. Photosynthesis and acquisition of carbon is based on BIOME3 (Haxeltine and Prentice, 1996a). Stomatal conductance is optimized to maximize carbon assimilation while simultaneously minimizing water loss. Net assimilated C is allocated to four crop compartments: root, stem including mobile reserves, leaves and storage organs. Yield is represented by the amount of C in storage organs. In this study, LPJmL operates on 0.5° grid cells (approx. 50 km at the equator) with individual land-use fractions and irrigation shares. Sowing and harvesting dates for crops are calculated internally considering climatic histories (Waha et al., 2012). LPJmL uses a potential productivity scaling factor accounting for management differences between countries: LAI_{max}, the maximum Leaf Area Index the plant can achieve under optimum conditions, ranging between 1 and 7 (Fader et al., 2010). This factor is calibrated per country and crop such that temporally averaged national yield levels simulated by LPJmL (including damages from ozone) and reported by FAO (FAO, 2016) agree (SI Figure S1).

We consider two staple crops, wheat and soybean, which together cover 22% of the global harvested area (Portmann et al., 2010). Since Asian and European/North American ("Western") wheat varieties are known to react differently to ozone (Emberson et al., 2009; Feng et al., 2012) we separately consider these two types (though the reasons for this difference are currently not known). Asian wheat is assumed as dominant in all countries east of 40° Eastern longitude (plus Turkey). For soybean this distinction is not made since differences are currently unclear (Emberson et al., 2009). A choice between spring and winter wheat is computed internally by LPJmL, depending on climatic suitability with a preference for winter wheat: spring wheat is only sown when winters are too cold or long, that is mostly in high Northern latitudes (Bondeau et al., 2007).

For the global runs, we applied a limited irrigation scheme: only water that is actually available for irrigation (after extraction of water necessary for household, industry and livestock) can be applied (Schaphoff et al., 2018). This is important particularly in South Asia where irrigation share is high, but available water limits effective crop irrigation (Elliott et al., 2014; Zampieri et al., 2018).

2.2 Modeling ozone effects

The complex interaction of ozone with crops is simplified to three steps in our model (Figure 1, Table 1). First, O_3 outside the leaf ($O_{3,out}$) is taken up via the stomata, leading to an inner-stomatal concentration $O_{3,in}$. Stomatal conductance for O_3 is derived from the conductance for water vapor by using a factor of 0.58 (dividing by 1.6, the difference in diffusion coefficients of CO_2 and water vapor, (Haxeltine and Prentice, 1996a) and by 1.075 to account for differences between CO_2 and O_3 (Ewert and Porter, 2000)). The concentration of O_3 in cells is virtually zero (Ewert and Porter, 2000; Plöchl et al., 2000), as other oxidizing agents (reactive oxygen species, ROS) are quickly formed. We do not resolve these intermediate reactions for

the sake of model simplicity, but subsume from now on all ozone-derived ROS as O_x. Second, $O_{x,in}$ is lowered by a detoxification process in cells and cell walls (Castagna and Ranieri, 2009; Plöchl et al., 2000) that dynamically reduces $O_{x,in}$ to a potentially harmful concentration $O_{x,harm}$. This process is split into two parts: an amount of $O_{x,in}$ is scavenged at no additional cost to the plant owed to a basal, un-targeted rate of antioxidants production (Blokhina et al., 2003; Jaleel et al., 2009), while the remaining fraction requires energy to be detoxified and thus increases the amount of carbon lost to maintenance respiration (Dizengremel et al., 2008; Ewert and Porter, 2000; Franz et al., 2017; Fuhrer et al., 1997). Franz et al. (2017) state that about half of external O_3 is taken up and detoxified via non-stomatal pathways (Kollist et al., 2000; Tuzet et al., 2011; Yin and Struik, 2009) and that this O_3 destruction pathway is important when assessing risks for plants. We do not directly account for these non-stomatal effects, but consider them as captured by the stomata-dependent detoxification. Though this may be oversimplified, in particular since the non-stomatal disposal of ozone depends on weather conditions or leaf age, we argue that the additional parameters necessary for a dynamic detoxification aside the stomata, i.e. when both stomatal and non-stomatal pathways are explicitly considered, are intractable with few experimental measurements only (note that an explicit calibration is not performed by Franz et al. (2017)). Moreover, we assume the core dynamics of detoxification, i.e. a fractional disposal of ozone before damage accrues, as sufficiently captured with a single pathway in our model, containing both basal (passive) and respiration-driven (active) detoxification. We do also not explicitly account for damage recovery, which is particularly relevant for younger leaves (Ewert and Porter, 2000), but subsume this effect in the detoxification process. We assume this as valid surrogate since damage repair requires energy as well. Since LPJmL employs a big-leaf approach, the distinction between younger and older leaves is currently also not possible. Third, the inner harmful concentration $O_{x,harm}$ induces damages: gross photosynthesis is reduced (short-term

damage) and senescence starts earlier (long-term), thereby shortening the time to acquire biomass and yield. The day of senescence onset is earlier for both wheat and soybeans, but the total growing time until maturity is not altered by ozone. Maturity is not advanced due to contrasting evidences or dose-dependent effects with low study coverage from the literature (Feng et al., 2008; Feng et al., 2011; Finnan et al., 1998; Pleijel et al., 1997; Zhu et al., 2011). The rate of senescence, i.e. the speed of decay, is not increased in our model, also due to ambiguous literature results (Dermody et al., 2006; Finnan et al., 1998; Pleijel et al., 1997). These three steps are added to the existing photosynthesis model (Table 1). Potential damages of O_3 to stomatal functioning (Hoshika et al., 2015; Mills et al., 2009), which would affect O_3 uptake in the long term, are not considered due to data scarcity for crops. Similarly, the direct sensing of O_3 by stomata, with subsequent closure independent of photosynthesis (Lombardozzi et al., 2012), is not simulated due to data scarcity. CO_2 fertilization of crops is considered in LPJmL (Bondeau et al., 2007; Haxeltine and Prentice, 1996a; Haxeltine and Prentice, 1996b) and affects the response of crops to O_3 via its effect on stomatal conductance: higher concentrations of CO_2 result in lower stomatal conductance, which in turn allows less O_3 to enter the leaves. The two molecules therefore act as antagonists: the more there is of one, the less the other will diffuse into leaves since both can lower stomatal conductance.

After calculating an optimized stomatal conductance that accounts for temperature, water, ozone and CO_2 concentration, the final daily C assimilation, C allocation and evapotranspiration are derived. All other steps in LPJmL are as described in Bondeau et al. (2007).

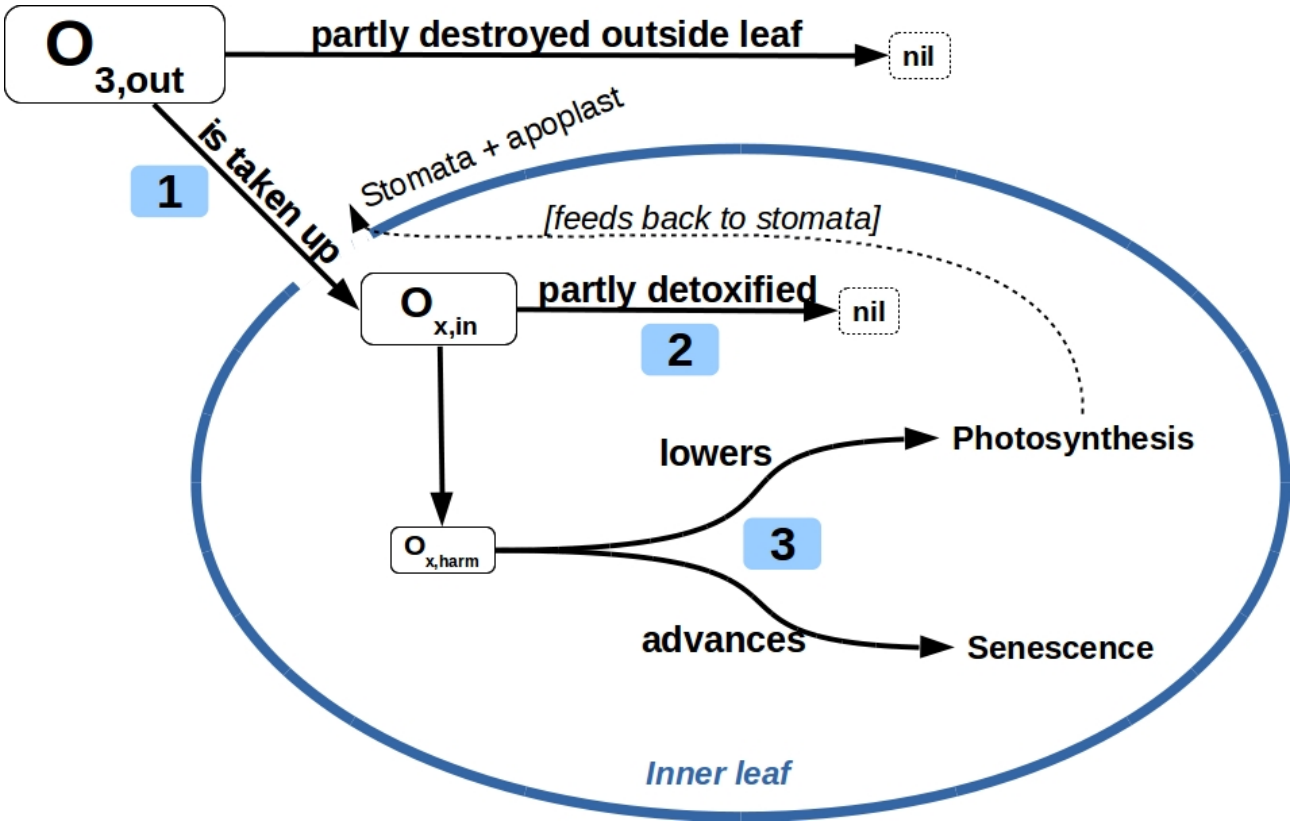

***Figure 1**: Reaction scheme of ozone as modeled in LPJmL. The size of $O_{3/x}$ boxes reflects their relative concentrations. Numbers refer to the three steps as described in text and Table 1. Symbols are $O_{3,out}$: outer ozone concentration, $O_{x,in}$: inner ozone/oxidative agent concentration (accounting for the fact that O_3 concentration inside cells is virtually zero), $O_{x,harm}$: harmful inner concentration, nil: non-oxidative reaction products. The dashed arrow from photosynthesis to stomata indicates a feedback, lowering stomatal aperture as a consequence of reduced photosynthesis.*

***Table 1**: Relevant equations in LPJmL to account for ozone stress. Units are omitted for clarity; see SI Table S2 for all symbols and units.*

Step	**Process**	**Affected variable**	**Relevant code lines**	**Explanation**
1	Uptake	Stomatal conductance	$\lambda = \min(\lambda(\text{water}; CO_2), \lambda(O_3; CO_2))$	Lambda (λ) is the relation between inner and outer [CO_2] with a maximum of 0.8. Water-limited and O_3-limited lambda are separately optimized, then the minimum of these two is taken to represent stomatal conductance[1].
		Inner [O_3]	$O_{x,in} = O_{3,out} * \lambda / \lambda_{max} * gc_{max}$	Relation between inner and outer O_3 depends on stomatal conductance, represented by λ over λ_{max} (0.8) times the maximum conductance under no stress.
2	Detoxification	Basic scavenging	$O_{x,inR} = \max(0, O_{x,in} - bs_{PFT})$	A certain amount of O_3 (or other ROS) is not harmful for the plant and is scavenged without additional energy costs (as detoxifying agents are assumed as basally present).
		Respiration	$rd = b_{C3} * V_{max} * (1 + r_{PFT} * O_{x,inR})$	The remaining O_x (i.e. O_3 or other ROS) increases cell respiration, for repairing and scavenging.
		Harmful [O_3]	$O_{x,harm} = O_{x,inR} * (1 - d_{PFT})$ $O_{x,harm.cum} = O_{x,harm.cum} + O_{x,harm}$	O_x is reduced by a percentage to the remaining harmful concentration. The cumulative harmful concentration $O_{x,harm.cum}$ is calculated (set to 0 at sowing).
3	Damage	Reduction of photosynthesis	$jc = c_{C3} * V_{max} * \max(0, 1 - j_{PFT} * O_{x,harm})$	Rubisco-limited photosynthesis *jc* is reduced by O_x. See also comments on V_{max} in the discussion.
		Senescence onset	Senescence starts when $PHU_{sum} / PHU_{max} > fracsen$; with $fracsen = 0.7 * \max(0, 1 - s_{PFT} * O_{x,harm.cum})$	Advancing of senescence is realized by lowering the phenological heat unit (PHU) threshold necessary to reach senescence (fracsen). The value of 0.7 (equal for wheat and soybeans) is the fraction of maximum attainable heat units (PHU_{max}) necessary for senescence onset under no ozone.

[1] The interaction between water stress and O_3 would best be represented by a hyperplane; but evaluation data is too sparse for an interactive response.

2.3 Parameter calibration

The ozone module requires five crop-specific parameters: bs_{PFT} (in mmol/m^2/day) describing the basal scavenging without energy cost, d_{PFT} (between 0 and 1, unitless) describing the fraction of $O_{x,in}$ that is detoxified at the cost of higher respiration, r_{PFT} (mmol^{-1}m^2 day) describing the respiration increase for this detoxification, j_{PFT} (mmol^{-1}m^2 day) describing the Rubisco (i.e. ribulose 1,5-bisphosphate carboxylase/oxygenase)-limited photosynthesis reduction due to ozone and s_{PFT} (mmol^{-1}m^2) describing the advance in senescence. No literature values were available for these five parameters, but they result as a compromise between our global focus and the harmonization of differently available measured variables across studies. Parameters were subjected to a calibration aiming to reproduce experimental studies. After a first round of calibration, where all five parameters were free, it became obvious that there are pairwise inverse correlations that require some parameters to be kept constant. We decided to fix bs_{PFT} and r_{PFT} , to which the model is either not very sensitive (r_{PFT}, Figure 4) or there is a reference value that can be derived from the literature (bs_{PFT}). We fixed bs_{PFT} at 0.16 mmol m^{-2} day^{-1}, corresponding to a threshold of non-damaging O_3 concentration of 40 ppbv (as in the AOT40 exposure metric often used in ERF studies, e.g. Avnery et al. (2011) or Fuhrer et al. (1997)) at a maximum stomatal conductance of 6 mm sec^{-1} (equal to 0.162 mol m^{-2} sec^{-1} of conductance to O_3 at 25°C and 1000 hPa pressure) for 8 hours (SI Table S3). The fixed value of r_{PFT} was determined by a linear regression using experiments (SI Table S1). Other crop-specific parameters like base temperatures or allocation constraints were not calibrated since these are based on literature values (Bondeau et al., 2007). No scaling from leaf to plant was used, i.e. the whole plant was treated as one big leaf.

Calibration was performed by traversing a full three-dimensional cube with 20 values for each of the three parameters to be calibrated (d_{PFT}, j_{PFT}, s_{PFT}), resulting in a total of 20^3 = 8,000

model runs per crop. Values were iterated, ranging from 0.05 to 5.0 times of the starting value (j_{PFT}, s_{PFT}) derived from linear regressions using experimental evidence, or between 0 and 100% (d_{PFT}). The weighted average root mean square error (RMSE) was used as target function, calculated for all pairs of observed and simulated variables. Growing-season averages (for model and experiment) were used if the measurement time point or the phenological phase was not clearly indicated in the studies. Weights for calibration variables were: 2 for the O_3 flux to leaves, 2 for relative stomatal conductance, 1 for A_{sat} as percentage of control, 1 for relative yield loss and 0.1 for respiration. Stomatal conductance and ozone uptake were weighed highest since these are the decisive processes that allow an upscaling from experimental to global level. Reduction in A_{sat} and relative yield loss are of second weighting since these are used as a mixture of result (from ozone uptake) and independent observation. Respiration was weighed least since experimental values were rare (see comments in SI Table S1). Resulting RMSE values were often similar (difference only in the third or fourth decimal place) such that of the 100 simulations with the lowest RMSE values the parameter set with the lowest reduction factors was chosen. This is justified by lower observed damages in reality than in experiments (Morgan et al., 2003). The LAI_{max} management parameter was adapted for each experiment before calibration such that the control yield level was correctly simulated.

The Web of Science® (http://apps.webofknowledge.com) was searched in spring 2016 for experimental studies that described ozone effects on wheat or soybean and reported one or more physiological observations useful for calibration (yield loss, O_3 uptake, light-saturated photosynthesis, stomatal conductance, respiration and/or growing season length). Six different studies containing 16 experiments were considered for Western wheat, seven studies with 12 experiments for Asian wheat and four studies with 11 experiments for soybeans (SI Table

S1). The experimental conditions described in these studies, including in particular O_3 and CO_2 concentrations, water provision and temperature, were provided as input for LPJmL. Output variables for comparison were extracted from the manuscripts, involving the use of the software *Engauge Digitizer* (Mitchell et al., 2018).

An out-of-sample calibration was performed to evaluate the reliability of the calibration process. Every study, each containing several measurements, was omitted from calibration in turn and the best parameters identified for the reduced experiment set. Simulation results for the experiments from the omitted study were then calculated with the out-of-sample calibrated parameters. The omission of studies corresponds to a 14-25% cross validation since each study contains at least two experiments (SI Table 1).

2.4 Ozone data

The ideal ozone data set for this exercise would contain observed daily, global surface O_3 concentrations over several years at 0.5° spatial resolution. But such a data set does not exist. Therefore we used an ensemble of daily global surface ozone concentrations, derived from chemical transport models participating in the ACCMIP model inter-comparison (Lamarque et al., 2013) and HTAP2 atmospheric pollution (Stjern et al., 2016) projects. Six models are included in the ensemble, all providing hourly or daily ozone concentrations: GEOSCCM, GFDL-AM3, MIROC-CHEM (all from ACCMIP), CHASER_re1, EMEP_rv48, GEOS-Chem (all from HTAP2). For either of the two experiment sets, an ensemble median was calculated pixel-wise, resulting in a total of eight global daily ozone input fields (six models plus two ensembles). Common available years for all models are 2008 to 2010. The usage of model ensembles is motivated by a better agreement of ensemble than single-model values with observed data (Fiore et al., 2009).

Hourly data were aggregated to daily data by averaging concentrations between 8 am and 4 pm. The daily values (aggregates or directly provided by the model) were downscaled from model resolution to 0.5° spatial resolution with a double-conservative remapping that conserves spatial gradients. A comparison of both ACCMIP and HTAP2 ensembles to observed values is shown SI Figure S2. Crop loss estimates were calculated with a reference of zero ozone and additionally with a scenario when all anthropogenic emissions (except methane) were reduced by 20%. Ozone data for the latter were provided by the HTAP2 "GLOALL" simulations (for 2010 only), for the three HTAP2 models included here.

2.5 Climate and land-use data

Temperature, precipitation, shortwave and longwave solar radiation are taken from the WFDEI data set (Weedon et al., 2014). These data have often been used by climate change impact models (Warszawski et al., 2014), and in particular in the Agricultural Model Intercomparison and Improvement Project's (AgMIP) global gridded crop model inter-comparison, GGCMI (Elliott et al., 2015).

Crop-specific land-use and irrigation fractions are extracted from the MIRCA2000 data set on 0.5° spatial resolution, representative of the global crop distribution around the year 2000 (Portmann et al., 2010). These fractions are held fixed to limit potential co-variation of O_3 damages and land-use shifts.

2.6 Model evaluation

Four levels of model evaluation were applied. First, the model was tested against experimental observations. These studies were also used to calibrate model parameters, once with the full data set and once as an out-of-sample calibration. Second, sensitivity runs were

performed where either input variables or model parameters were varied. These runs were not compared to observations, but gave insights whether the inner mechanics of the model were reasonably adherent to the modelled processes. Third, simulated national yield losses were compared to previous studies by McGrath et al. (2015), Ghude et al. (2014) and Burney and Ramanathan (2014). Fourth, the global historical loss estimates produced by LPJmL were compared to previous estimates using Exposure Response Functions (ERFs), which linearly relate ozone exposure above a threshold to crop losses.

3. Results

3.1 Parameter calibration

The calibration procedure leads to crop-specific parameter sets (Table 2). Asian and Western wheat parameters differ in detoxified percentage, photosynthesis decrease and respiration increase; all of them show larger effects of O_3 on Asian wheat. Calibration plots for each crop (Figure 2) show the agreement between experimentally observed and simulated values for ozone uptake, light-saturated (i.e. Rubisco-limited) photosynthesis A_{sat}, stomatal conductance for water and yield loss. For each of the variables different counts of observations are available. Out-of-sample calibration shows that the results are robust towards omission of several experiments (SI Figure S3). Stomatal conductance and ensuing ozone uptake show variation around the 1:1 line, but no systematic bias, and largely match with observations in dynamics and magnitude. Note that ozone uptake is not measured for any experiment with Asian wheat. Relative yield loss is estimated rather conservatively for all three crops – there is no simulation below the 1:1 line.

***Table 2**: Calibrated values for the five O_3 parameters*

Parameter	Western wheat	Asian wheat	Soybeans	Comment
bs_{PFT}	0.1600	0.1600	0.1600	Fixed value
d_{PFT}	0.7395	0.6353	0.7395	
r_{PFT}	0.1000	0.1729	0.9470	Fixed value
j_{PFT}	0.0100	2.6874	0.568	
s_{PFT}	0.0844	0.0896	0.0323	

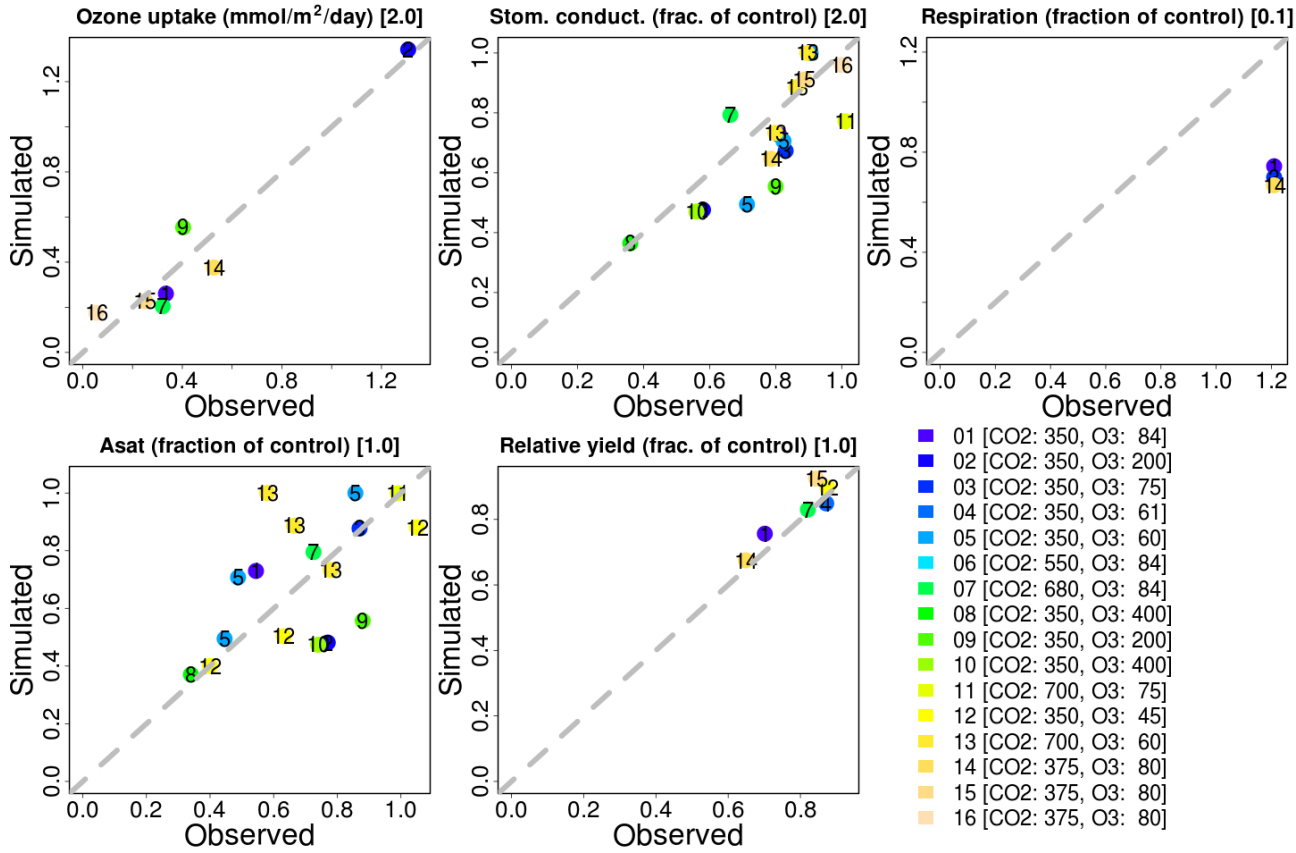

(a) Western wheat

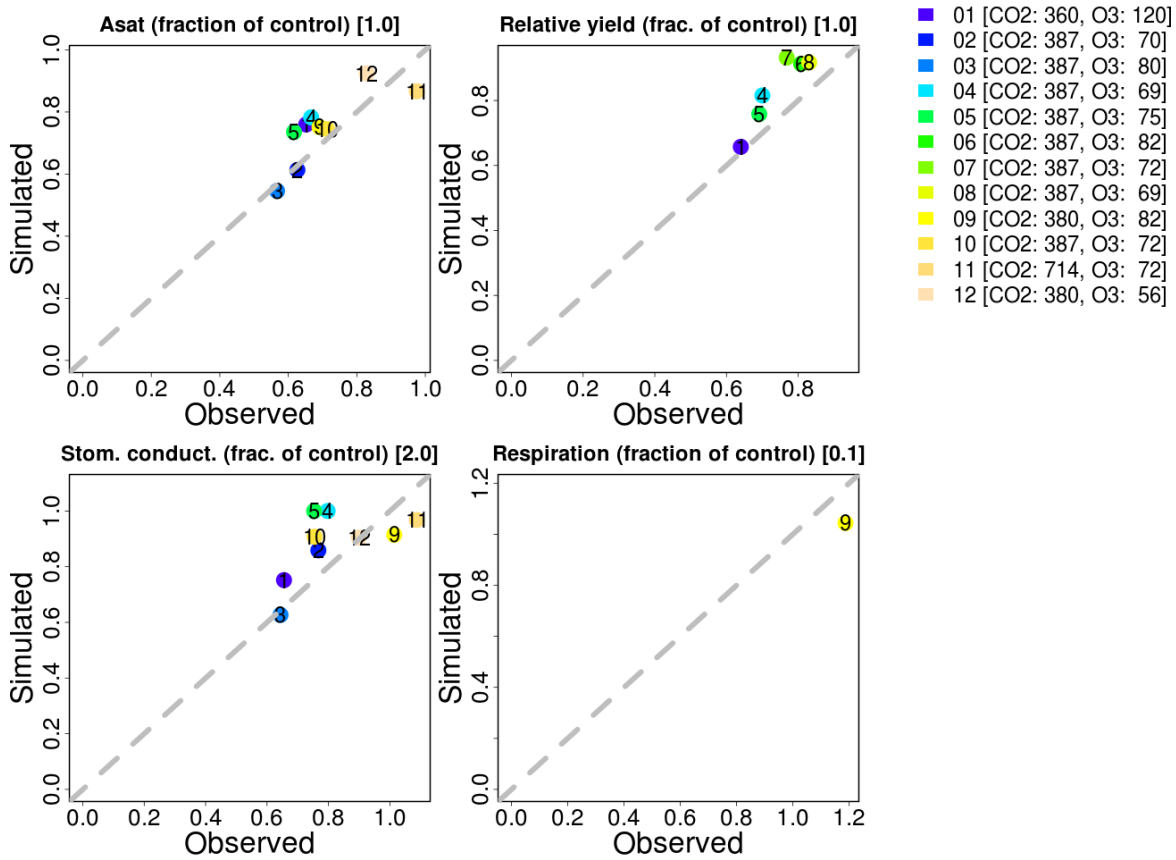

(b) Asian wheat

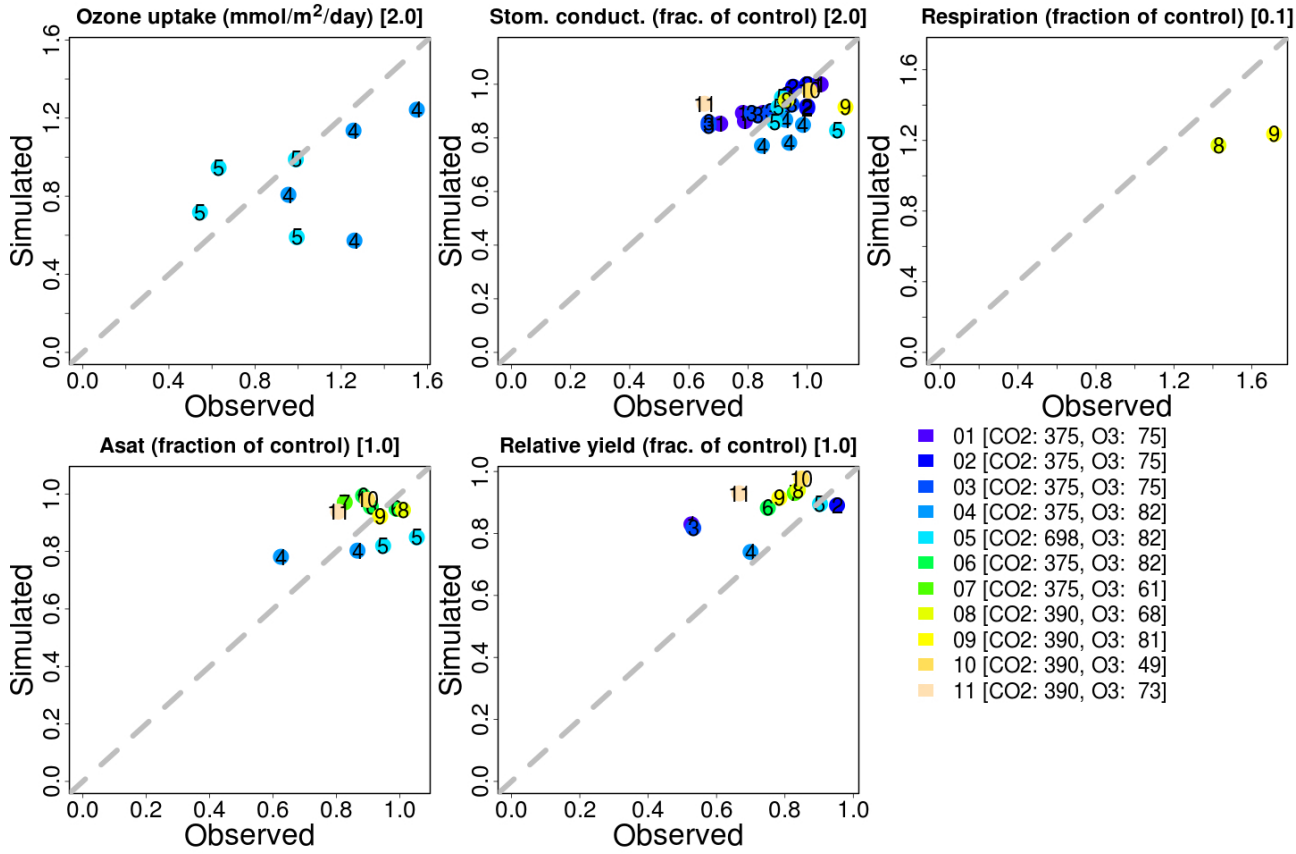

(c) Soybeans

Figure 2*: Calibration results for* ***(a)*** *Western wheat,* ***(b)*** *Asian wheat,* ***(c)*** *soybeans. Subpanels show experimentally observed values on the x-axis and simulated values on the y-axis. Different colors denote different experiments; detailed descriptions are listed in SI Table S1. There can be several measurements of one variable within one experiment. Ideally all points would lie on the 1:1 line shown for comparison. Numbers in brackets in sub-captions denote calibration weights (see Methods).*

3.2 Sensitivity towards weather or parameter variation

Sensitivity of the model towards input variation is displayed in Figure 3 and SI Figure S4, similar to the tests conducted by Ewert and Porter (2000). Response dynamics of three key variables (light-saturated photosynthesis A_{sat}, stomatal conductance and ozone uptake) are evaluated under different growth conditions for one example day during late leaf expansion or early senescence. Variations include ozone concentration, exposure time, CO_2 concentration and precipitation. Temperature and illumination were simulated as optimal and repeated each day. All crops convey similar dynamics (SI Figure S4). Since phenological development, in particular when the LAI changes with development, influences photosynthetic performance, analogous plots without senescence advancing can be found in SI Figure S5. This exercise with ozone-unaffected senescence onset conveys similar patterns as the original analysis (except ozone uptake monotonically increasing with exposure time).

Light-saturated photosynthesis (A_{sat}) increases with higher CO_2, but high O_3 concentrations dampen this increase (Figure 3; SI Figure S4). The relative loss in A_{sat} in reference to O_3-free conditions is, however, levelling off with higher CO_2. Stomatal conductance is reduced by a higher load of either CO_2 or O_3. At high O_3 and low CO_2 concentrations simulated stomata are completely closed. The influence of O_3 diminishes with higher CO_2 concentrations. Closely connected to stomatal conductance is O_3 uptake, which decreases with higher CO_2 but increases with higher O_3.

Scarcity of water leads to a less important role of O_3, evidenced by smaller differences between A_{sat}, conductance and O_3 uptake at low water levels. Both relative and absolute photosynthetic damages increase with water provision. For high O_3 loads stomatal conductance levels off: it does not increase with more water to avoid excess O_3 uptake.

Longer O_3 exposure times lead to higher O_3 uptake and thus lower A_{sat} and stomatal conductance. Stomatal conductance, A_{sat} and O_3 uptake turn down to zero at high levels of O_3.

The day of senescence onset slightly advances with higher management intensity (SI Figure S6). Simulated plant growth (LAI) and development (as relative phenology) are influenced by atmospheric ozone (SI Figure S7).

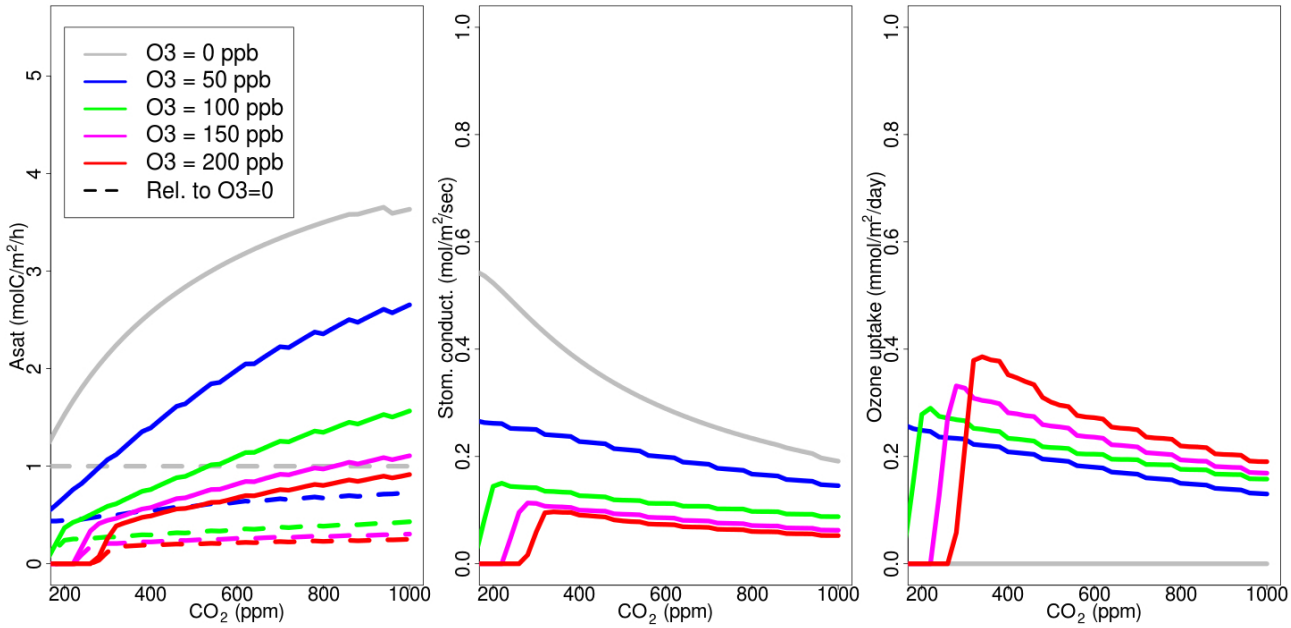

(a) Varying CO_2 concentrations, at 8 hours of exposure and 6mm daily precipitation

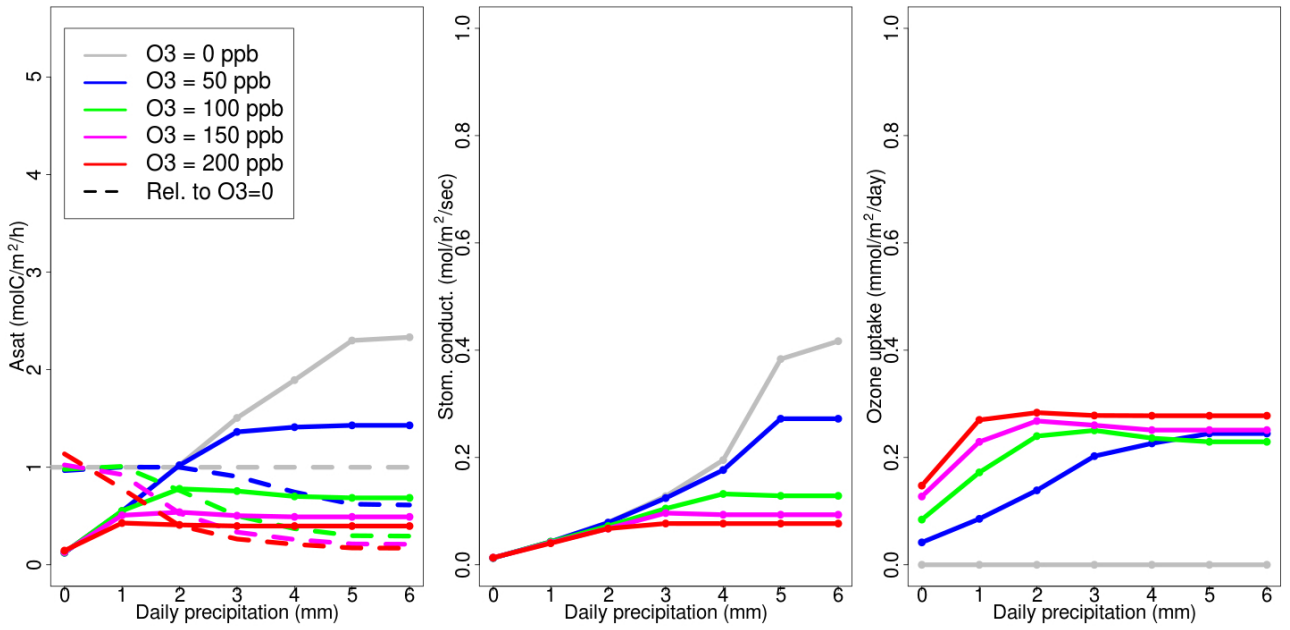

(b) Varying precipitation levels, at 8 hours of exposure and CO_2 at 340 ppm

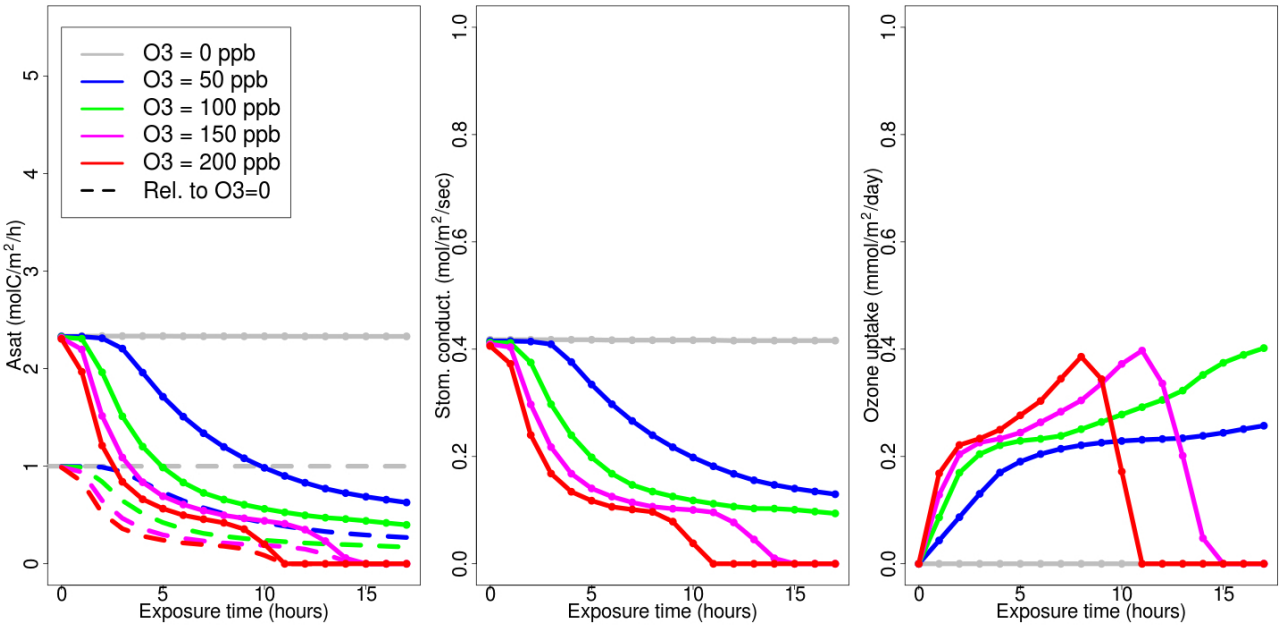

(c) Varying exposure times, at 6mm daily precipitation and CO_2 at 340 ppm

Figure 3*: Sensitivity of crop responses against varying inputs of* ***(a)*** *CO_2 concentration,* ***(b)*** *water supply and* ***(c)*** *ozone exposure times for Asian wheat (for other crops see SI Figure S4). Data are taken as one-day snapshots at mid growing season (81 days after sowing, which is in the leaf expansion phase for ozone doses up to 50 ppb, but already in senescent phase for the others – see also SI Figure S7). The response of A_{sat}, stomatal conductance and O_3 uptake is shown. Different colors denote different ozone concentrations.*

Model sensitivity towards varying ozone parameters, at constant weather and O_3 conditions, is shown in Figure 4. The five ozone-related parameters were varied between +/- 90% of their calibrated or fixed values. Simulated yields react most to changes in the detoxified fraction (d_{PFT}) of O_3: the more is detoxified, the higher are yield values. The second largest sensitivity is found towards senescence advancing (s_{PFT}); then follows the basal scavenging (bs_{PFT}). The Rubisco-limited photosynthesis reduction factor (j_{PFT}) shows impact only for Asian wheat, while the respiration increase factor (r_{PFT}) shows an influence only for soybeans. Sensitivities with parameters fixed at low, rather than mean, reduction factors are shown in SI Figure S8. These show distinct responses and orders of parameters, but underlining the choice of d_{PFT},

s_{PFT} and j_{PFT} as calibration parameters. Basal scavenging would exert measurable influence on yields, but was fixed as this is the only parameter that can be tied to literature values (see Methods).

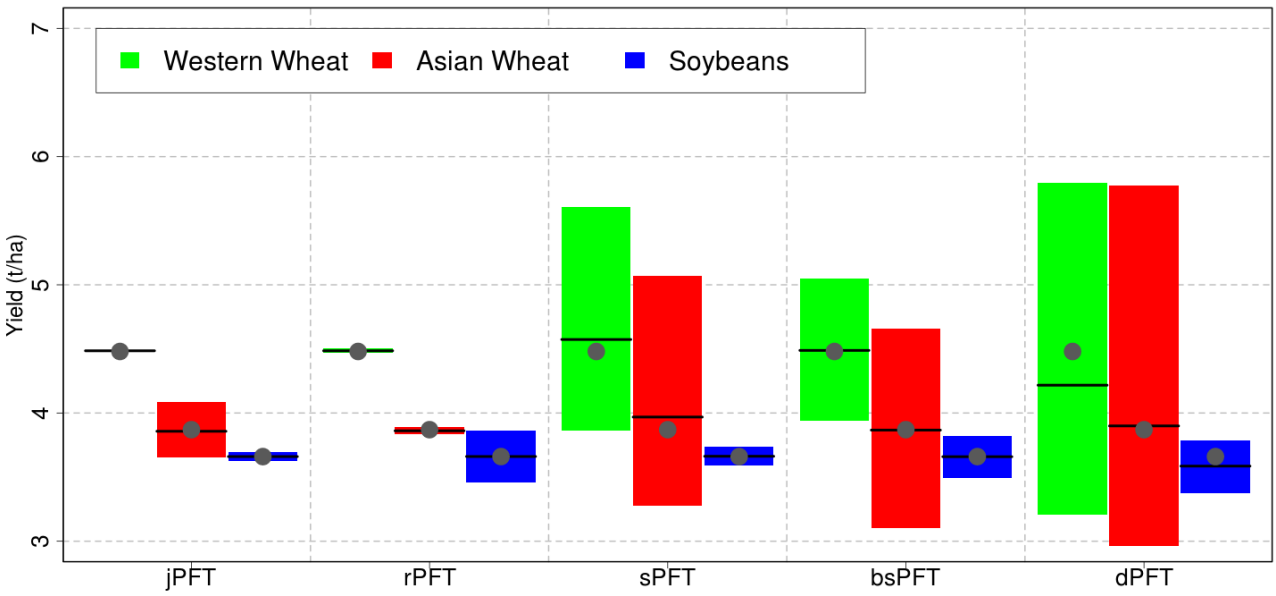

Figure 4*: Sensitivity of simulated yields against perturbed crop parameters. Each of the five parameters was varied from -90% to +90% of its calibrated value (Table 2, except that d_{PFT} was limited to a maximum of 100%); the other four parameters were held at their calibrated values. Black lines indicate mean yield values across all parameter values; grey dots indicate yields when all parameters are held at their calibrated/fixed values. Constant optimal temperature, precipitation and illumination were used (details see SI Figure S8).*

3.3 Historical yield losses

Historical global yield loss due to ozone pollution between 2008 and 2010 was calculated with LPJmL. Mean ozone levels during summer, based on the ACCMIP model ensemble, are displayed in Figure 5. These range from 7 ppbv in Amazonia and Papua-New Guinea up to more than 60 ppbv in the Middle East. Eastern US and Europe, in particular Italy, are stricken by high O_3 levels (50-60 ppbv) in the summer season. This suggests that major crop producing regions, which are mostly in the Northern Hemisphere, are substantially affected by O_3 pollution.

Maps of relative losses, separately for rainfed and irrigated yields, referring to a hypothetical scenario with zero surface ozone are shown for Western wheat (Figure 6), Asian wheat (Figure 7) and soybeans (Figure 8). Both wheat types are simulated globally for comparison. The (unrealistic) scenario with zero surface ozone was chosen for ease of comparison with two previous global studies, Van Dingenen et al. (2009) and Avnery et al. (2011),

Irrigated yields (with irrigation limited by available water) show more pronounced relative losses than rainfed yields for all crops. Western wheat losses range from 0 to 25% for rainfed yields, with high losses in Central Europe, followed by the Eastern US (Figure 6). Irrigated Western wheat yield losses range between 5 and 35%, with low spatial variation within main producing areas. Globally, land-use weighted wheat losses were estimated at 5.4% for rainfed and 15.1% for irrigated yields, if all planted wheat was of Western type.

Asian wheat losses range between 0 and 30% for rainfed and 10-50% for irrigated crops (Figure 7). The highest losses occur in India, Pakistan and China where ozone load is high and a substantial fraction of crops is irrigated. Globally, land-use weighted wheat losses were estimated at 9.8% for rainfed and 25.6% for irrigated yields, if all planted wheat was of Asian

type.

Relative yield losses for soybeans range between 0 and 13% for rainfed crops, where the highest reductions are observed in the Balkans and Eastern US (Figure 8). Reductions for irrigated soybeans are up to 15% in several regions, in particular in Northern China, Iran and the US Midwest. Globally, land-use weighted soybean losses are estimated at 3.8% for rainfed and 8.0% for irrigated yields.

Nationally aggregated yield losses due to ozone pollution are shown in Figure 9. Only the top producers (cumulatively accounting for at least 90% of global production between 2000 and 2011, split between Asian and Western wheat) for each crop are considered. Uncertainties in the estimation due to different O_3 model inputs are shown by black (ACCMIP) and blue (HTAP2) lines. Mean losses for Western wheat range from 1-3% in Argentina, Australia or Canada to up to 23% in France and 27% in Egypt. For Asian wheat mean losses range from 4-6% in Iran and Turkey up to 39% in India. Soybeans show mean losses between 2% in Argentina and 10% in China. The uncertainty range due to O_3 concentrations is around 11% of the mean loss, averaged over all crops, models and countries. Differences between countries are usually due to different levels of O_3 pollution, water limitation or management intensities, which affect canopy conductance, and different matches of crop growing season and peak ozone load. Since an atmospheric ozone concentration of zero is not realistic, a similar loss assessment was performed where all anthropogenic emissions (except methane) were reduced by 20% in 2010, relative to observed levels. Loss ranges are much lower in this case (SI Figure S9).

Yield losses estimated with LPJmL were compared to two previous global assessments based on exposure-response functions. In Van Dingenen et al. (2009) and Avnery et al. (2011) the

authors each compile a global ozone field for the year 2000, using a chemical model, and estimate yield losses with previously published ERFs for wheat and soybeans based on two different ozone damage indices. A comparison of the loss estimates is provided in Table 3. For LPJmL the mean across all eight ozone inputs is supplied while for the ERF studies the mean from both indices is shown. Losses for soybeans are estimated consistently lower by LPJmL, with Latin America as the only exception. Loss estimates for wheat deviate from the ERF studies, too, but not in a consistent direction.

Table 3*: Comparison of relative yield losses between previous estimates and LPJmL. Exact regional definitions can be found in the two ERF studies. Western and Asian wheat parameters for LPJmL are denoted with [W] and [A].*

Crop	**Region (Country)**	**Loss by ERF:** Van Dingenen et al. (2009)	**Loss by ERF:** Avnery et al. (2011)	**Loss by LPJmL**
Soybeans	North America	12.4%	14.4%	10.2%
	Latin America	n.a.	3.3%	3.8%
	Europe	23.9%	25.6%	10.7%
	Africa & Middle East	n.a.	5.9%	1.7%
	China / East Asia	16.1%	22.8%	6.2%
	India / South Asia	11.9%	8.2%	5.3%
	Oceania	n.a.	1.9%	1.9%
Wheat	North America [W]	4.3%	6.8%	3.9%
	Latin America [W]	n.a.	3.7%	1.4%
	Europe [W]	4.4%	7.7%	14.2%
	Africa, Mid-East [W, A]	n.a.	13.0%	6.1%
	China / East Asia [A]	14.4%	9.8%	34.2%
	India / South Asia [A]	20.4%	17.4%	36.7%
	Northern Asia [A]	n.a.	6.9%	6.4%
	Oceania [W]	n.a.	0.5%	0.0%

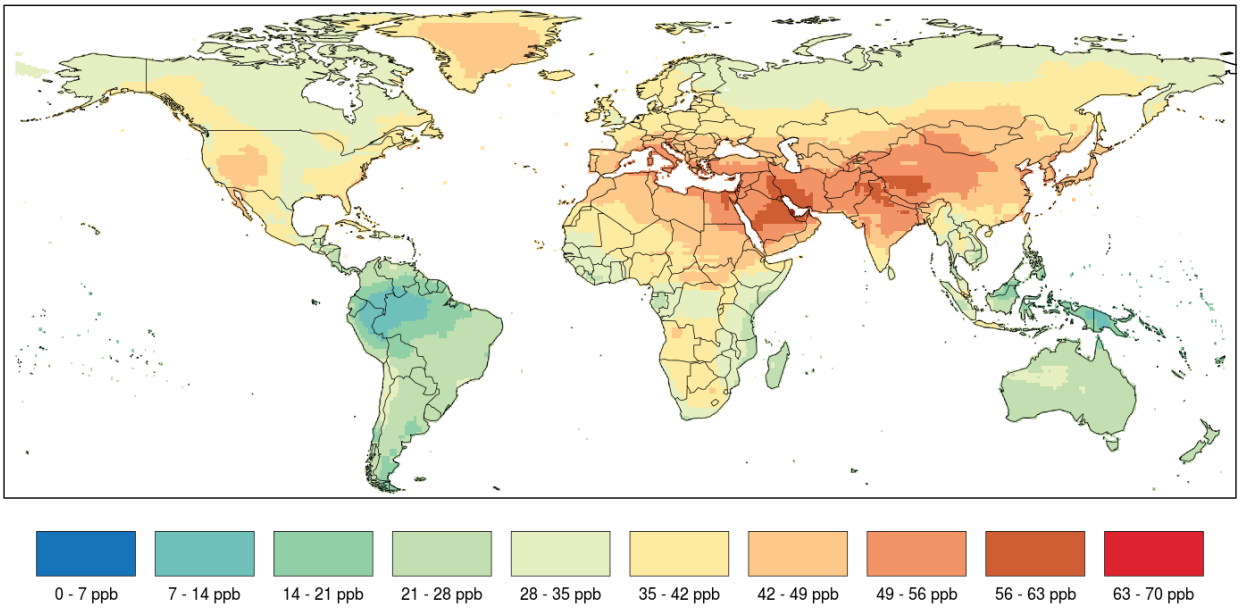

***Figure 5**: Means of daily ozone levels in ppbv, averaged between 2008 and 2010 during the summer growing season, derived from the ensemble of ACCMIP models. Growing season is defined as April to August on the Northern and December to April on the Southern Hemisphere.*

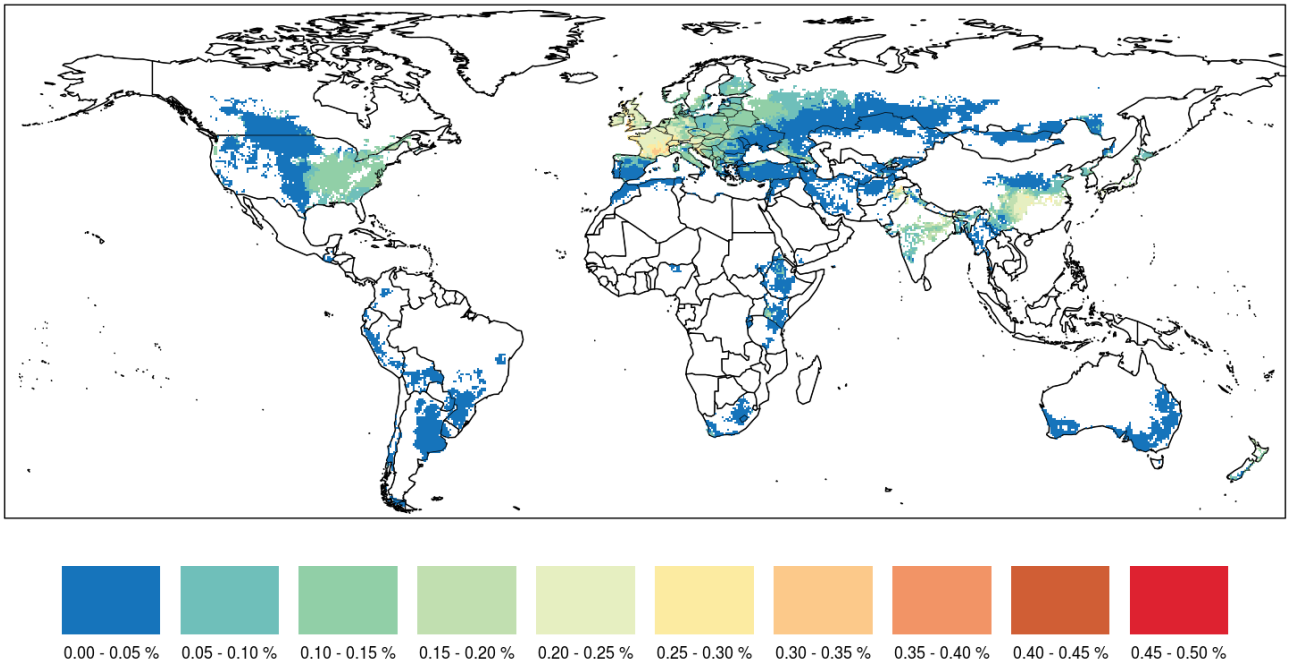

(a) Rainfed

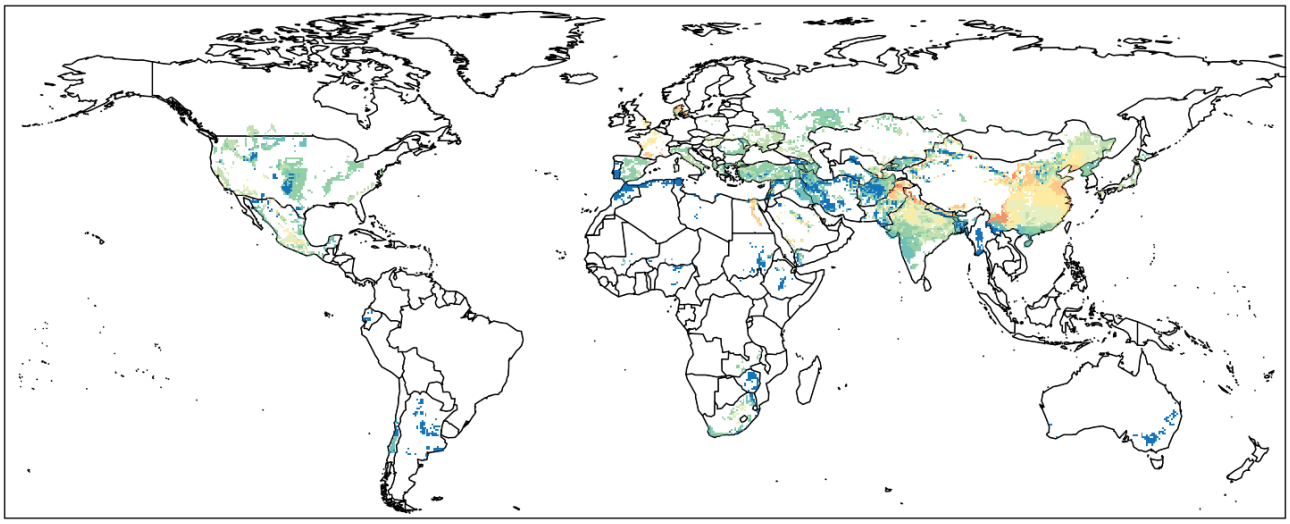

(b) Irrigated

Figure 6*: Historical Western wheat yield losses as fraction of unharmed yields at zero O_3. White areas have no cropping area in MIRCA2000. Panels show* ***(a)*** *rainfed and* ***(b)*** *irrigated yields. The ACCMIP model ensemble was used as O_3 input.*

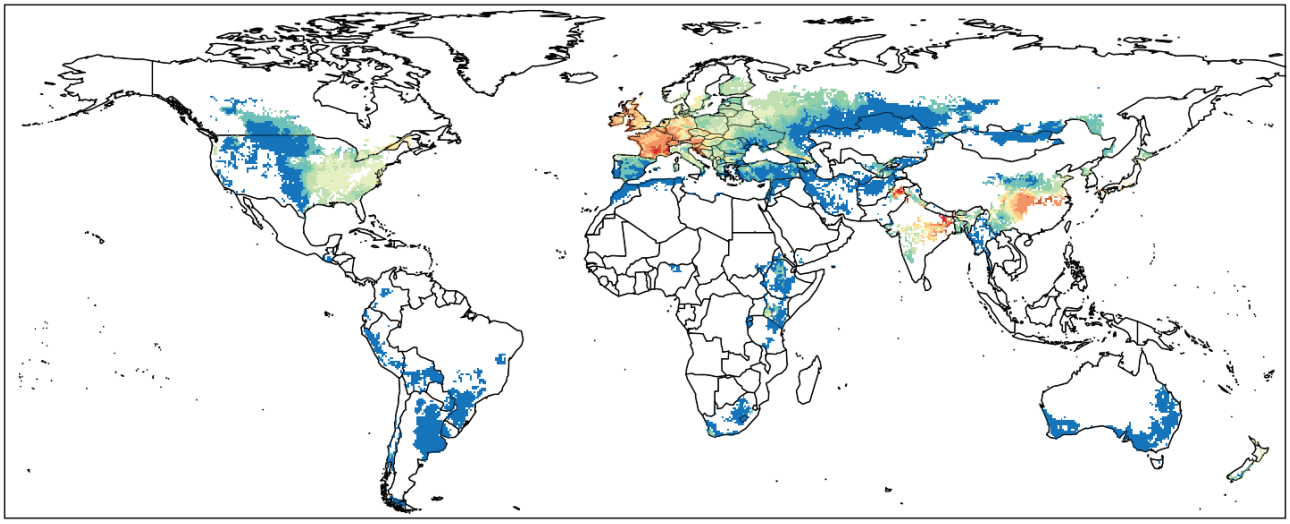

(a) Rainfed

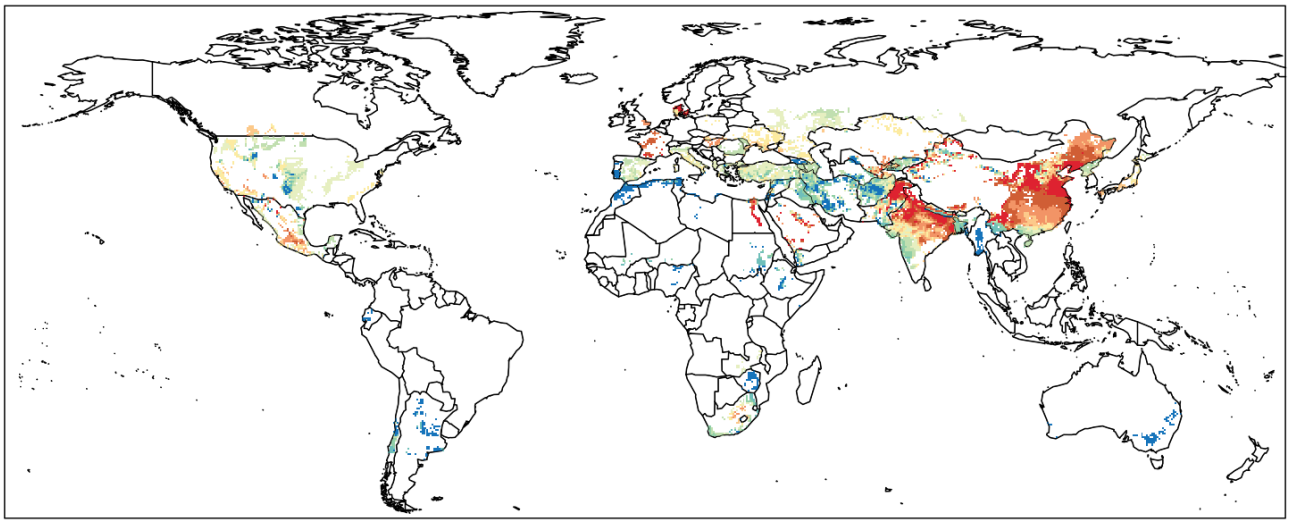

(b) Irrigated

Figure 7*: As Figure 6, but for Asian wheat (same color scale).*

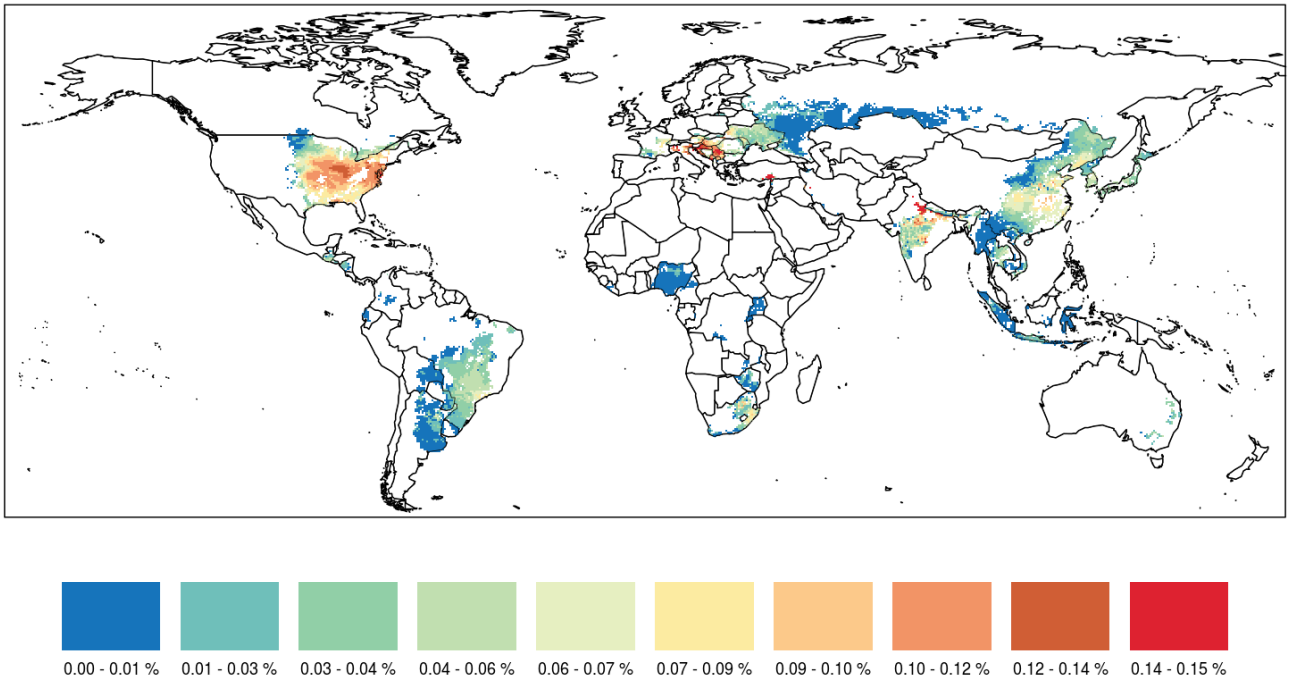

(a) Rainfed

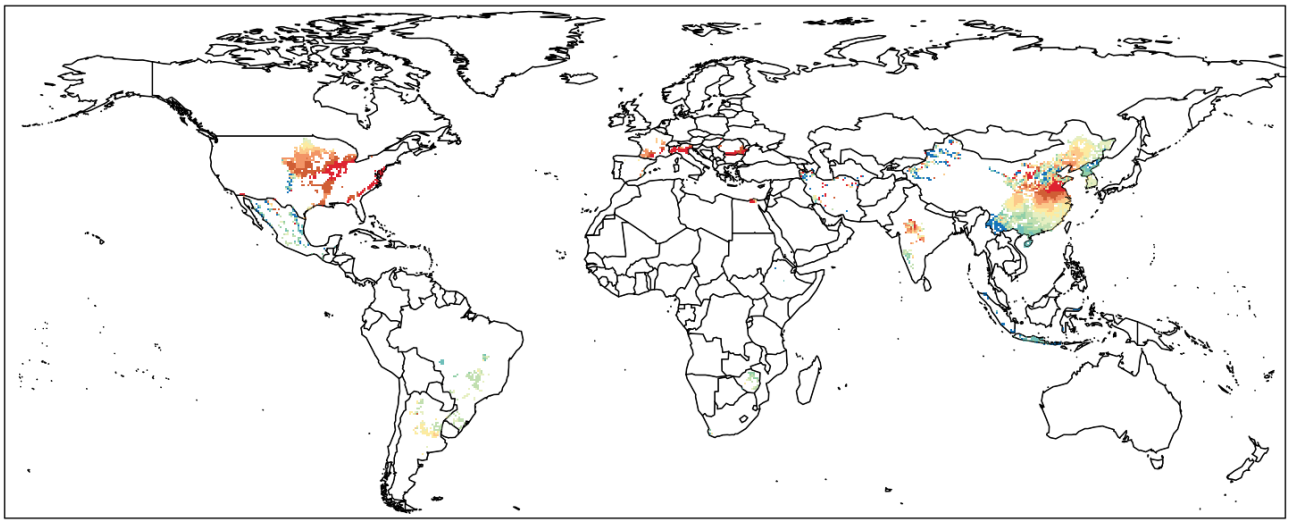

(b) Irrigated

Figure 8*: As Figure 6, but for soybeans.*

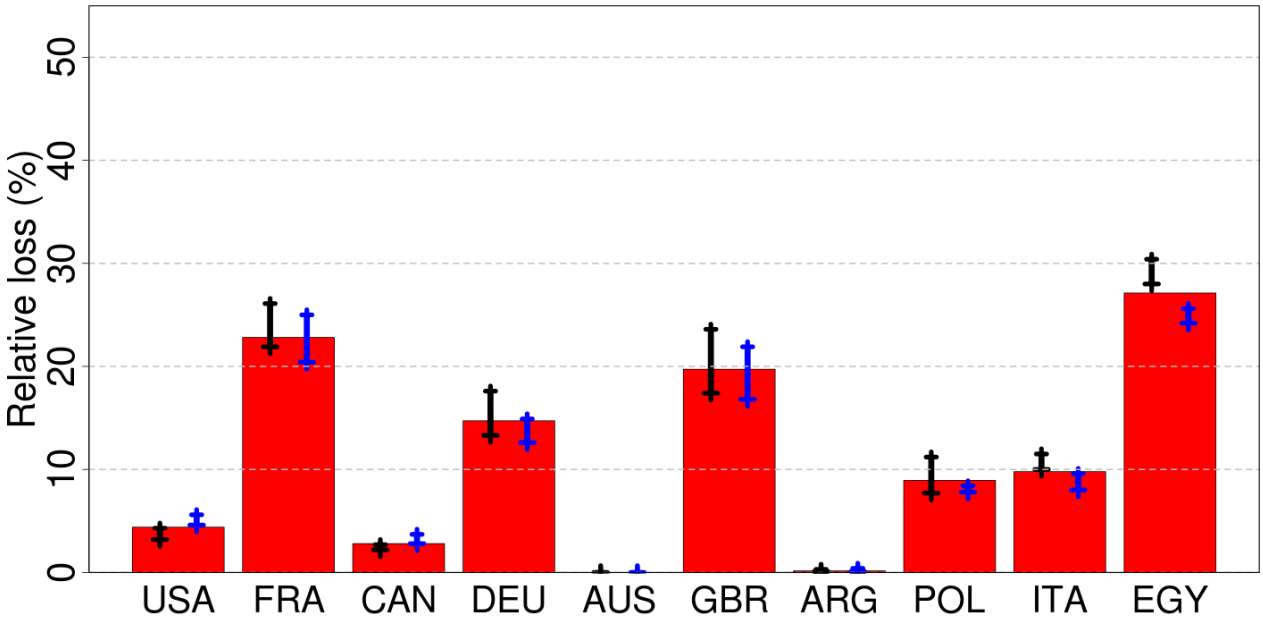

(a) Western wheat

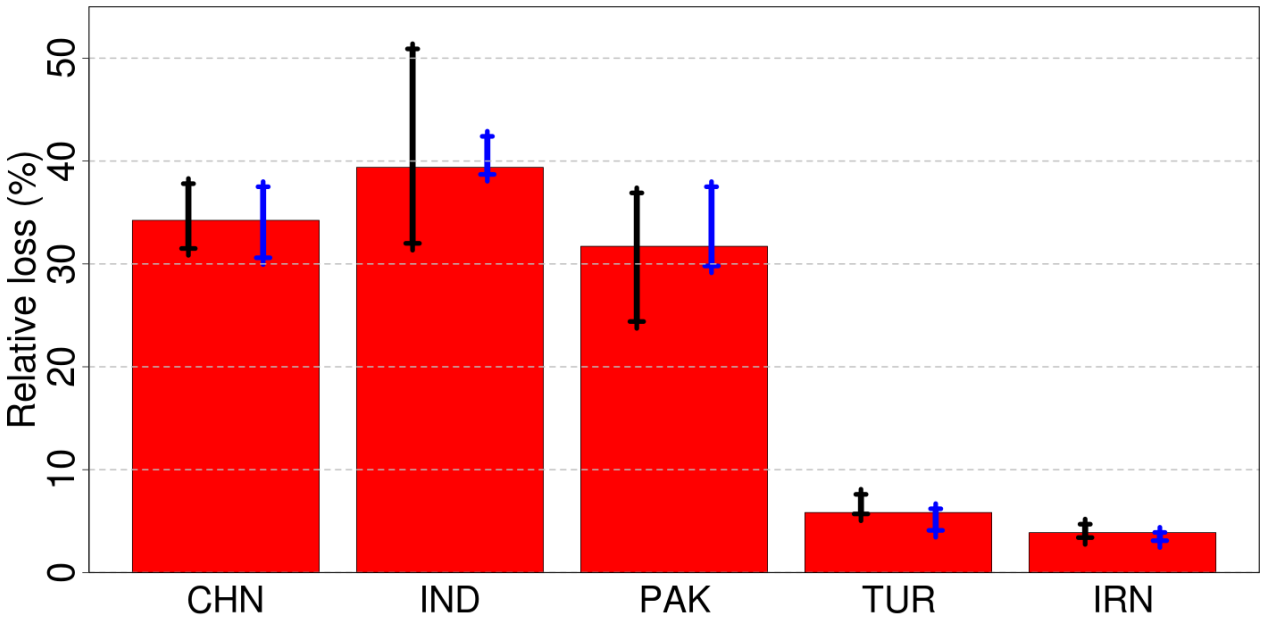

(b) Asian wheat

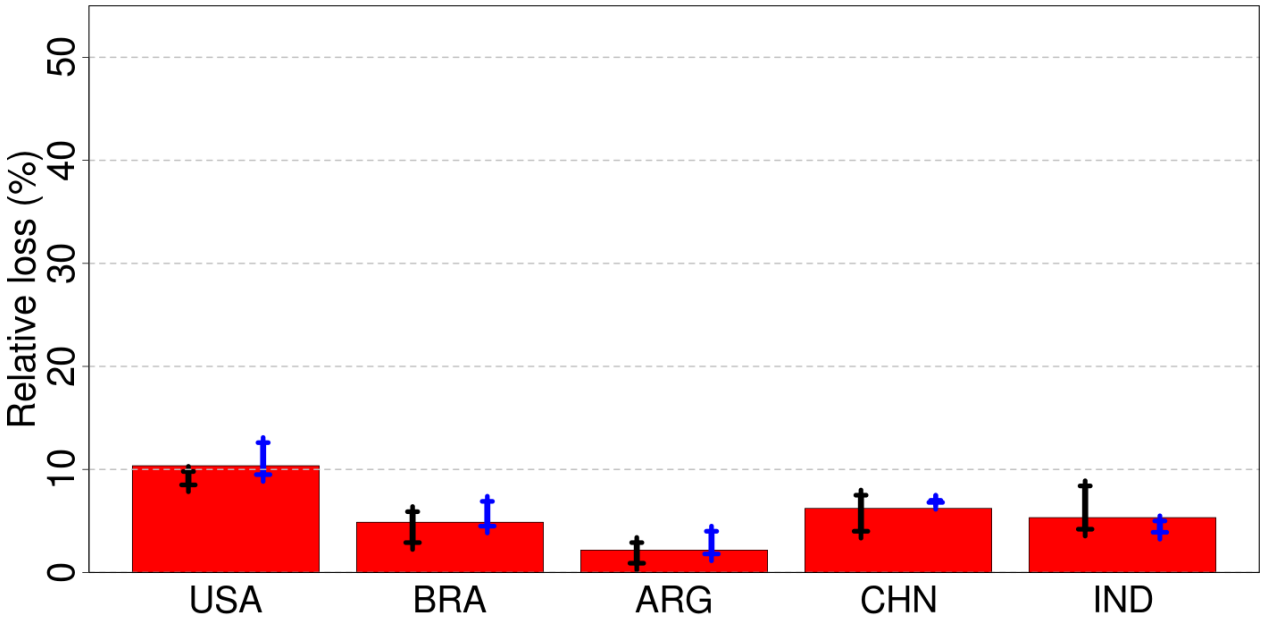

(c) Soybeans

Figure 9*: Nationally aggregated yield losses due to ozone, relative to zero pollution, for the main producers of each crop:* ***(a)*** *Western wheat,* ***(b)*** *Asian wheat,* ***(c)*** *soybeans. Red bars show yield losses as land-use weighted averages over all grid cells with at least 0.05% land-use share of the respective crop, as the mean of eight different global* O_3 *input fields (see Methods). Black lines show loss ranges among ACCMIP models, while blue lines show loss ranges among HTAP2 models. Countries are ordered by total production. Yield losses with*

respect to a 20% reduction of emissions (instead of zero ozone) are shown in SI Figure S9.

4. Discussion

We have implemented a novel ozone damage module into the widely used global crop model LPJmL. Parameters were calibrated to experiments and with these we have estimated global historical yield losses. Losses range from virtually 0% up to 40% and agree with previous yield loss estimates in several cases. This study is the first to consider water stress, temperature, management intensity and CO_2 concentration as co-variates of ozone effects at the global level within a crop model. To account for distinct sensitivities to O_3, Western and Asian wheat were simulated separately.

4.1 Model design

Simulating ozone damages with a process-based model is more complex than regressions between yield and accumulated pollutant exposure as in ERFs. But mechanistic descriptions offer several advantages: capturing non-linear effects on sub-seasonal scale, accounting for variation in ozone response due to variable water supply or temperature and including the antagonistic role of O_3 and CO_2. Our equation design is based on a diverse literature background and was tailored for seamless integration into the LPJmL framework. Yet there are several caveats concerning the formulation. First, the earlier onset of senescence, but an unaffected rate of senescence or maturity day may contradict with some experimental observations (though there is no consensus; see Methods). But a reducing effect of O_3 on active LAI is visible with this approach (SI Figure S7a), which we deem sufficient for our aims in this study. Second, previous approaches implemented a decrease in photosynthesis from ozone by reducing V_{max}, the CO_2-limited maximum rate of carboxylation, as observed by experiments (Farage and Long, 1995). We chose to reduce the Rubisco-limited photosynthesis rate jc instead of V_{max}, as observed in Betzelberger et al. (2012), since

respiration in LPJmL is linearly dependent on V_{max} (Haxeltine and Prentice, 1996a) and would therefore decrease with higher O_3 load. However, a decrese in respiration has not been observed in experiments – respiration increases with O_3 (Feng et al., 2008). Third, LPJmL utilizes a big-leaf approach to scale from molecular processes to ecosystem level. This simplification neglects differential effects of O_3 on young and old leaves or other plant parts (Ewert and Porter, 2000), but is deemed necessary for the global scale. Fourth, a direct impact of O_3 on stomata apart from the coupling via photosynthesis effects (Lombardozzi et al., 2012) is not considered since no data are available for crops. Fifth, the amount of ozone that is scavenged without any effect on the plant may change over time or in stressful conditions when ROS defense mechanisms may also be required under, for example, drought stress (Ewert and Porter, 2000; McGrath et al., 2015). This is not considered due to lacking data on crops. Sixth, damage repair is not explicitly considered but subsumed with detoxification for the sake of model simplicity. This is inaccurate, though, since repair capacities diminish with leaf age (Ewert and Porter, 2000). Seventh, the daily time step may be too coarse to capture non-linear impacts of sub-daily ozone peaks. We account for this uncertainty by calibrating model parameters for daily time step simulations. Overall, we developed an ozone damage module of intermediate complexity that does not capture sub-daily, leaf-specific effects but runs swiftly, globally and accounts for co-variates like temperature and water. The level of detail for capturing ozone effects on crops suggested by Emberson et al. (2018) is thus only partly fulfilled. Of their recommendations we do, specifically, consider daily variations in stomatal conductance, timing of ozone peaks during the growing season, influences of management (dynamic growing seasons, spring/winter cultivar choice and irrigation) and interaction with climate and CO_2. But our model does not include leaf-specific dynamics (stomatal conductance and repair capacity dependent on leaf age), differential effects during particularly sensitive times during the growing season like anthesis, sub-daily variations in

ozone and stomatal conductance or a variable harvest index (see also the seven points above). Note, though, that it is recognized also by Emberson et al. (2018) that the necessary experimental data set to calibrate a model of such depth are yet to be identified. Therefore we consider our ozone module as a first step towards more advanced modelling of physiological effects. Recently, new model types have been proposed accounting for the phytotoxic ozone dose (POD) i.e. the effectively damaging amount of O_3 entering the plant, which consider stomatal conductance and phenology in a simplified way (Mills et al., 2018a; Mills et al., 2018b) and are thus preferable over purely exposure-based damage functions (Mills et al., 2011). Yet our module, integrated in a larger vegetation model, in principle allows for an integral study of advanced research questions for the following reasons. The simulation of ozone damage is directly coupled with plant growth which is, in turn, dependent on phenology, dynamic soil water content, allocation of photosynthates to plant compartments and available nutrients. The use of daily climate information allows for non-linear responses over the growing season, for example when vernalization requirements for winter wheat have not been met. Furthermore, an interaction with other vegetation (e.g. weeds) is, in principle, possible. A particular example for the advantage of an integrated crop model is to consider the modulating effect of actually available irrigation water on ozone damages, as demonstrated in this study.

4.2 Parameter calibration and sensitivity

The high model sensitivity towards the detoxified fraction is due to its influence on all downstream processes (respiration, photosynthesis, senescence). Basal scavenging is an additive reduction and therefore does not show as large an influence as the respiration-driven detoxification d_{PFT}. Precocious senescence displays substantial influence on yields since it deprives the plant of radiation interception twice: less new leaves are formed and the existing ones are less active. The sensitivity towards parameters depends on crop and absolute

parameter value. Therefore the parameters can only be interpreted as a complete set since they are dependent on each other and the rather few experimental observations do not allow for an unambiguous quantification of mechanisms. This suggests that possibly a more simple reduction of net photosynthesis by a combined factor (including respiration changes) would also be sufficient, as long as further experimental constraints are not available. Calibration is more reliable for experiments that measure several considered target variables simultaneously (e.g. experiments 4 and 5 for soybeans) than for experiments with only few observed variables.

Though dynamics of stomatal conductance, ozone uptake and photosynthesis response are captured by the model, there is a bias towards lower yield losses in the model than observed in experiments. This bias is small for Western wheat and concerns only some experiments for Asian wheat, but is more substantial for soybeans. The three experiments with the highest deviation (numbers 1, 2, and 11; Figure 2) show, however, unusually high yield losses within the experiments for a given O_3 concentration (SI Figure 10). Therefore the deviance of LPJmL from these observations is not considered problematic. The agreement between previous and our national soybean loss estimates indicates that this underestimation in experiments is not present under large-scale conditions, for which LPJmL is designed.

The usage of a global model with parameters that have been calibrated with point-based experiments may entail uncertainties. This concerns management, weather or unobserved influences on yields that are not resolved at larger scales. We aimed to limit these uncertainties by using different types of experiments with varying locations and conditions. Experimental results should also be treated with caution since among them there is uncertainty in the magnitude of ozone effects (Bernacchi et al., 2006). Therefore it is reasonable to allow some error in the reproduction of experimental observations as long as

these are unbiased and the dynamic range – large response differences from largely different conditions – is captured.

The association of predominant wheat type (Western or Asian) with country in our study is arbitrary and does not account for differences within each group. Additionally, except the ozone factors, all other crop parameters – which are derived from literature and intended to cover a broad range of wheat-type cereals like barley or rye (Bondeau et al., 2007) – are kept constant, which may not reflect physiological reality. But the different values for ozone factors after calibration, with higher penalties for Asian wheat, and the agreement with previous studies of coherently larger losses in Asia support the geographical split into two types. Yet hypotheses about physiological reasons for the different response, e.g. a particularly sensitive photosynthesis in Asian types, cannot be deduced in the light of the current uncertainties with a global model.

4.3 Sensitivity towards input data

Simulated responses to different climate conditions agree with expectations. The antagonistic roles of O_3 and CO_2 (Bernacchi et al., 2006; Ewert and Porter, 2000) and the protective role of water deficit against O_3 damage (at the price of generally lower yields) are captured. Higher ozone loads or longer exposure also lead to more damage, as expected.

Absolute and relative yield losses depend on management intensity. Management including fertilizer, cultivar choice or pest control is reflected only by the parameterized maximum leaf area index (LAI_{max}) in LPJmL (Fader et al., 2010), since the utilized version does not contain explicit nitrogen cycles or pest dynamics. Therefore the correct adjustment of management in the model is of salient importance (SI Figure S1). Experimental evidence also suggests that a

scaling of losses with better management is reasonable, in particular when leading to higher stomatal conductance (Biswas et al., 2008). LAI_{max} was separately scaled for each country and crop between 1 and 7 such that national average yield levels between 2008 and 2010 (the time frame with available ozone data) match between LPJmL simulations and FAO reported yields (Fader et al., 2010). The calibration considers reported ozone values to avoid implicit ozone damage in the national management settings when atmospheric concentrations are altered in an experiment. Calibration at national level does not account for within-country differences in production intensity, as is the case e.g. in France or the US. We argue, however, that comparisons between nations are nonetheless possible, in particular when considering that the required time series of sub-national yield data are not everywhere available (Ray et al., 2012). An earlier onset of senescence with higher LAI_{max} (SI Figure S6) can be expected, since better plant growth allows ozone damage to accumulate faster.

4.4 Reliability of ozone input data

We compared monthly ozone data, derived from hourly or daily ozone concentrations from six models, to the observational data set provided by Sofen et al. (2016); see SI Figure S2. Both ACCMIP and HTAP2 ensembles tend to overestimate low monthly ozone pollution, in particular in northern latitudes. Reasons for this bias are discussed in Fiore et al. (2009), Schnell et al. (2015), Guo et al. (2018) and Solazzo et al. (2017). A local-mean-based bias correction was attempted for our study, but did not alter results much (data not shown). The existing uncertainties in ozone modeling require more sophisticated methods for correction, which we did not aim for in this study. A study on pollution-related mortality (Fang et al., 2013) used ozone inputs with a similar bias as our ensemble. Therefore we used the uncorrected single models and ensembles, assuming to cover uncertainties regarding ozone input by this approach.

Ozone input was assumed as static in our study, i.e. daily concentrations are not modified by uptake or dry deposition. An atmospheric coupling between transpiration, vapor pressure deficit and uptake of CO_2 or O_3 would be necessary to capture the full dynamics of this complex process. This is currently not included in any crop model and requires interaction between biosphere and atmosphere models. Thus we assume static ozone fields as sufficient to assess national yield losses due to ozone.

4.5 Comparison to previous loss estimates

Our loss estimates for rainfed soybeans largely agree in magnitude with previous results. The LPJmL-based loss estimate for total US soybeans is 10.4% (range is 8.5 to 12.6%). For only rainfed yields this figure is 10.1% (8.2-12.3%), and for only irrigated yields 13.1% (11.7-15.6%). The value estimated by LPJmL is therefore double the value of 5.5% for rainfed US soybeans provided by McGrath et al. (2015), possibly due to an overestimation of ozone concentration in the US (SI Figure S2). Indian soybean yield loss estimates by LPJmL are 5.3% (3.9-8.4%), corresponding in magnitude with the 2.7% (+/- 1.9%) estimated by Ghude et al. (2014). For Indian wheat, there is agreement in the range of losses between LPJmL with 39.4% (32.0-50.9%) and the study by Burney and Ramanathan (2014), who estimate 40% (20-60%, depending on the state). Note that Burney and Ramanathan (2014) consider black carbon and ozone together and do not feed concentrations but rather precursor emissions into their equations. Therefore estimates are not directly comparable. Loss calculations in Ghude et al. (2014), however, are eight-fold lower with 5.0% (+/- 1.2%). In that study, even the region most affected by ozone is estimated to suffer from only 17% yield loss. A possible reason for differences is water stress: LPJmL explicitly simulates the interaction of water and ozone, while most statistical studies use a linear relationship between ozone and yields under

all circumstances. A precipitation control is included in McGrath et al. (2015) and Burney and Ramanathan (2014), but not Ghude et al. (2014). This may explain the difference for wheat, which is mostly irrigated in India, and the better match for soybeans, which are dominantly rainfed in India. Therefore we conclude that the consideration of water availability is of importance when assessing ozone losses. There may even be an economic trade-off for irrigation when ozone load is high (Mills et al., 2018a; Mills et al., 2018b): more irrigation also leads to more ozone damage, such that the benefit of irrigation may just be leveled by the costs of ozone damage. This relationship has to be studied in more detail, though.

Our loss estimates agree only limitedly (Table 3) with the global studies by Avnery et al. (2011) and Van Dingenen et al. (2009). Possible reasons for differences are divergences in ozone concentration due to different chemistry models, the consideration of different years, no distinction between Asian and Western wheat types and, above all, the lack of water levels in their ozone response. This may lead to overestimation of losses in water-stressed regions but to an underestimation in well-watered regions. Other putative causes for differences include a possible mismatch between real and assumed growing seasons (for all three studies), a wrong adjustment of management settings with LAI_{max} in LPJmL or temperature effects on crops not considered in the ERF studies. Overall we assume loss assessments by LPJmL as a supplement to the previous estimates, not as a replacement. Although LPJmL integrates co-factors like temperature or water provision including its limited physical availability, the new approach also brings new uncertainties (see above) such that superiority of LPJmL over ERFs is not warranted. But for future assessments, where interaction between CO_2 and O_3 may play a larger role than today, or when soil dynamics or atmospheric couplings are of interest, LPJmL is better equipped for such simulations.

4.6 Historical loss estimations

The estimation of historical yield losses due to ozone pollution suggests that ozone is a major yield-reducing factor in several regions on the globe. This agrees with expectations founded on experimental findings and observed ozone pollution. Reduction on the field is usually less than in chambers due to protective effects of water status (Fuhrer, 1995), sub-daily timing (Heath et al., 2009), though not reflected in LPJmL, and a possible shift between growing season and peak ozone load, depending on crop and region (Van Dingenen et al., 2009).

LPJmL estimates relative yield losses from irrigated yields as consistently higher than from rainfed yields. This is due to a higher stomatal conductance allowing more ozone to penetrate. Several experiments have shown this relative protective effect of water deficit (Bou Jaoudé et al., 2008; Fuhrer, 1995; Khan and Soja, 2003). In McGrath et al. (2015), however, the authors find the opposite for rainfed soybeans in the US: losses are higher under dry conditions. They argue for a decoupling of stomatal conductance and water status by impaired abscisic acid (ABA) signaling. This eventually allows more ozone to enter under drought than under unstressed conditions, which aggravates losses. Another possible explanation for their finding could be that water-stressed plants have a limited capacity to detoxify ozone as antioxidant compounds are also necessary to combat drought consequences. Since neither model is currently able to resolve these processes, more detailed models and experimental studies are necessary to identify causes for differences.

Asian countries are simulated as particularly susceptible to losses for two reasons: higher pollution and higher sensitivity of crops (Emberson et al., 2009). The high loss estimation of 39% for wheat in India can be explained by combining these two factors and an almost exclusively irrigated cultivation, which allows for stomata to stay open and for more ozone to

enter. Yet this may be an overestimation given the sensitivity of the model towards management intensity and the uncertainty of ozone input data with very few observations in this region. Additionally, our simulations may still assume too much available water for irrigation since environmental flows are not considered here (Jagermeyr et al., 2017). Rather high reductions of around 20% for wheat in France, Germany and UK are unexpected, but may be reasonable in the light of substantial ozone pollution, limited water stress and high management intensity. Another explaining factor is the slight overestimation of ozone pollution in Western Europe by the ozone model ensemble (SI Figure S2). Finally, despite already high loss fractions and the considerations above, it is possible that LPJmL loss estimates are rather conservative given the deviation to lower losses when compared to experiments (Figure 2). Yield losses in similar ranges (averaged over country classes) have recently been provided by Mills et al. (2018a) and Mills et al. (2018b), indicating that substantial crop damage by ozone is plausible also in developed nations.

In our assessment a baseline of zero O_3 was used for comparison. This is unrealistic in practice since background biogenic emission of precursors, as well as contributions from the stratosphere, can hardly be mitigated. A more realistic estimate of *avoidable* ozone damage is therefore provided by the 20% emission reduction (corresponding to a globally averaged 3.3% reduction in ozone concentration) experiments in the HTAP2 simulations (SI Figure S9). These calculations still point to several percent of unnecessary yield sacrifices.

Further model developments could comprise the inclusion of C_4 crops like maize, the combination of O_3 effects with other pollutants like SO_2 or NO_2 (Rai et al., 2007) or other stressors similar to Mills et al. (2018b) or the usage of different cultivars and sensitivities. Further questions that can be answered are adaptation options (e.g. shifting growing season, using different cultivars, ozone-sensitive water management) or assessment of future losses

due to O_3. A coupled modelling between atmosphere, chemistry and biosphere would additionally allow for assessing the effects of O_3 mitigation more realistically.

4.7 Conclusion

Our implementation of a process-based global model to estimate historical yield losses from ozone has confirmed previous findings: major crop producers suffer from substantial production damage due to ozone pollution. Our research has emphasized that damaging effects are dependent on co-factors, in particular water status, which should be considered when establishing O_3 pollution thresholds. We consequently consider the inclusion of O_3 effects on crops as relevant for climate change impact studies, as climate change can alter water cycles, temperatures and ozone pollution. This would lead to modified yield expectations, with modifications possibly in a similar range as current uncertainties of crop projections (Rosenzweig et al., 2014). As a corollary of our assessment we propose that more surface ozone observation stations in particular in Asia, Africa and Latin America are established, as these regions are currently data scarce (Sofen et al., 2016) but suffer from ozone damage to crops.

Acknowledgements

We thank F. Wechsung, S. Szopa, D. Hauglustaine, J. Lathiere, Y. Balkanski and P. Ciais for helpful discussions and T. Bendixen for data provision. BS acknowledges funding from the German National Academic Foundation. SR and CM acknowledge financial support from the MACMIT project (01LN1317A) funded through the German Federal Ministry of Education and Research (BMBF). Author contributions: BS initiated, designed and performed the study and wrote the manuscript with contributions from all co-authors.

The authors declare to have no competing financial interests.

References

Ainsworth, E.a., Yendrek, C.R., Sitch, S., Collins, W.J. and Emberson, L.D., 2012. The Effects of Tropospheric Ozone on Net Primary Productivity and Implications for Climate Change. Annual Review of Plant Biology, 63(1): 637-661.

Avnery, S., Mauzerall, D.L. and Fiore, A.M., 2013. Increasing global agricultural production by reducing ozone damages via methane emission controls and ozone-resistant cultivar selection. Global change biology, 2013(19): 1285-1299.

Avnery, S., Mauzerall, D.L., Liu, J. and Horowitz, L.W., 2011. Global crop yield reductions due to surface ozone exposure 1. Year 2000 crop production losses and economic damage. Atmospheric Environment, 45(13): 2284-2296.

Bernacchi, C.J. et al., 2006. Hourly and seasonal variation in photosynthesis and stomatal conductance of soybean grown at future CO(2) and ozone concentrations for 3 years under fully open-air field conditions. Plant, cell & environment, 29(11): 2077-90.

Betzelberger, A.M. et al., 2012. Ozone exposure response for U.S. soybean cultivars: linear reductions in photosynthetic potential, biomass, and yield. Plant Physiol, 160(4): 1827-39.

Biswas, D.K. et al., 2008. Genotypic differences in leaf biochemical, physiological and growth responses to ozone in 20 winter wheat cultivars released over the past 60 years. Global change biology, 14.

Blokhina, O., Virolainen, E. and Fagerstedt, K.V., 2003. Antioxidants, Oxidative Damage and Oxygen Deprivation Stress a Review. Annals of Botany, 91: 179-94.

Bondeau, A. et al., 2007. Modelling the role of agriculture for the 20th century global terrestrial carbon balance. Global change biology, 13(3): 679-706.

Bou Jaoudé, M., Katerji, N., Mastrorilli, M. and Rana, G., 2008. Analysis of the ozone effect on soybean in the Mediterranean region. European Journal of Agronomy, 28(4): 519-525.

Broberg, M.C., Feng, Z., Xin, Y. and Pleijel, H., 2015. Ozone effects on wheat grain quality - A summary. Environmental Pollution, 197: 203-213.

Burney, J. and Ramanathan, V., 2014. Recent Climate and Air Pollution Impacts on Indian Agriculture. Proceedings of the National Academy of Sciences of the United States, 111(46): 16319-24.

Castagna, A. and Ranieri, A., 2009. Detoxification and repair process of ozone injury: from O3 uptake to gene expression adjustment. Environ Pollut, 157(5): 1461-9.

Chuwah, C., van Noije, T., van Vuuren, D.P., Stehfest, E. and Hazeleger, W., 2015. Global impacts of surface ozone changes on crop yields and land use. Atmospheric Environment, 2015(106).

Dermody, O., Long, S.P. and DeLucia, E.H., 2006. How does elevated CO2 or ozone affect the leaf-area index of soybean when applied independently? The New phytologist, 169(1): 145-55.

Dizengremel, P., Le Thiec, D., Bagard, M. and Jolivet, Y., 2008. Ozone risk assessment for plants: central role of metabolism-dependent changes in reducing power. Environ Pollut, 156(1): 11-5.

Elliott, J. et al., 2014. Constraints and potentials of future irrigation water availability on agricultural production under climate change. Proceedings of the National Academy of Sciences of the United States of America, 111(9): 3239-44.

Elliott, J. et al., 2015. The Global Gridded Crop Model Intercomparison: data and modeling protocols for Phase 1 (v1.0). Geoscientific Model Development, 8(2): 261-277.

Emberson, L.D., Ashmore, M.R., Cambridge, H.M., Simpson, D. and Tuovinen, J.P., 2000. Modelling stomatal ozone flux across Europe. Environmental Pollution, 109(3): 403-413.

Emberson, L.D. et al., 2009. A comparison of North American and Asian exposure-response data for ozone effects on crop yields. Atmospheric Environment, 43: 1945-1953.

Emberson, L.D. et al., 2018. Ozone effects on crops and consideration in crop models. European Journal of Agronomy.

Ewert, F. and Porter, J.R., 2000. Ozone effects on wheat in relation to CO2 Modelling short-term and long-term responses of leaf photosynthesis and leaf duration. Global change biology, 6: 735-750.

Fader, M., Rost, S., Müller, C., Bondeau, A. and Gerten, D., 2010. Virtual water content of temperate cereals and maize: Present and potential future patterns. Journal of Hydrology, 384(3-4): 218-231.

Fang, Y., Mauzerall, D.L., Liu, J., Fiore, A.M. and Horowitz, L.W., 2013. Impacts of 21st century climate change on global air pollution-related premature mortality. Climatic Change, 121(2): 239-253.

FAO, 2016. FAOStat, http://faostat3.fao.org/home/E.

Farage, P. and Long, S.P., 1995. An in vivo analysis of photosynthesis during short-term 03 exposure in three contrasting species. Photosynthesis Research, 43: 11-18.

Feng, Z., Kobayashi, K. and Ainsworth, E.A., 2008. Impact of elevated ozone concentration on growth, physiology, and yield of wheat (Triticum aestivum L.): a meta-analysis. Global change biology, 14.

Feng, Z., Pang, J., Kobayashi, K., Zhu, J. and Ort, D.R., 2011. Differential responses in two varieties of winter wheat to elevated ozone concentration under fully open-air field conditions. Global change biology, 17(1): 580-591.

Feng, Z. et al., 2012. A stomatal ozone flux–response relationship to assess ozone-induced yield loss of winter wheat in subtropical China. Environmental Pollution, 164: 16-23.

Finnan, J.M., Jones, M.B. and Burke, J.I., 1998. A time-concentration study on the effects of ozone on spring wheat (Triticum aestivum L.). 3: Effects on leaf area and flag leaf senescence. Agriculture, Ecosystems & Environment, 69: 27-35.

Fiore, A.M. et al., 2009. Multimodel estimates of intercontinental source-receptor relationships for ozone pollution. Journal of Geophysical Research, 114(D4).

Fishman, J., Ramanathan, V., Crutzen, P.J. and Liu, S.C., 1979. Tropospheric ozone and climate_Nature.pdf>. Nature, 282(5741): 818-820.

Franz, M., Simpson, D., Arneth, A. and Zaehle, S., 2017. Development and evaluation of an ozone deposition scheme for coupling to a terrestrial biosphere model. Biogeosciences, 14: 45-71.

Fuhrer, J., 1995. Critical Level for Ozone to Protect Agricultural Crops Interaction with Water Availability. Water, Air and Soil Pollution, 85: 1355-60.

Fuhrer, J., 2009. Ozone risk for crops and pastures in present and future climates. Naturwissenschaften, 96(2): 173-94.

Fuhrer, J., Skaerby, L. and Ashmore, M.R., 1997. Critical levels for ozone effects on vegetation in Europe. Environmental Pollution, 97(1): 91-106.

Gaudel, A. et al., 2018. Tropospheric Ozone Assessment Report: Present-day distribution and trends of tropospheric ozone relevant to climate and global atmospheric chemistry model evaluation. Elem Sci Anth, 6(1): 39ff.

Ghude, S.D. et al., 2014. Reduction in India's crop yield due to ozone. Geophysical Research Letters, 5685-91.

Guo, J.J. et al., 2018. Average versus high surface ozone levels over the continental U.S.A.: Model bias, background influences, and interannual variability. Atmospheric

Chemistry and Physics Discussions: 1-31.
Haxeltine, A. and Prentice, I.C., 1996a. BIOME3: An equilibrium terrestrial biosphere model based on ecophysiological constraints, resource availability, and competition among plant functional types. Global Biogeochemical Cycles, 10(4): 693-709.
Haxeltine, A. and Prentice, I.C., 1996b. A general model for the light-use efficiency of primary production. Functional Ecology, 10(5): 551-561.
Heath, R.L., Lefohn, A.S. and Musselman, R.C., 2009. Temporal processes that contribute to nonlinearity in vegetation responses to ozone exposure and dose. Atmospheric Environment, 43(18): 2919-2928.
Hoshika, Y. et al., 2015. Ozone-induced stomatal sluggishness changes carbon and water balance of temperate deciduous forests. Nature Scientific Reports, 5(May).
IPCC, 2013. Climate Change 2013: The Physical Science Basis. Contribution of Working Group I to the Fifth Assessment Report of the Intergovernmental Panel on Climate Change, Cambridge, United Kingdom and New York, NY, USA, .
Jagermeyr, J., Pastor, A., Biemans, H. and Gerten, D., 2017. Reconciling irrigated food production with environmental flows for Sustainable Development Goals implementation. Nature communications, 8: 15900.
Jaleel, C.A. et al., 2009. Antioxidant defense responses: physiological plasticity in higher plants under abiotic constraints. Acta Physiologiae Plantarum, 31(3): 427-436.
Khan, S. and Soja, G., 2003. Yield responses of wheat to ozone exposure as modified by drought-induced differences in ozone uptake. Water, Air and Soil Pollution, 147: 299-315.
Kollist, H., Moldau, H., Mortensen, L., Rasmussen, S.K. and Jørgensen, L.B., 2000. Ozone Flux to Plasmalemma in Barley and Wheat is controlled by Stomata rather than by direct Reaction of Ozone with Cell Wall Ascorbate. Journal of Plant Physiology, 156(5-6): 645-651.
Lamarque, J.F. et al., 2013. The Atmospheric Chemistry and Climate Model Intercomparison Project (ACCMIP): overview and description of models, simulations and climate diagnostics. Geoscientific Model Development, 6(1): 179-206.
Lin, M. et al., 2015. Climate variability modulates western US ozone air quality in spring via deep stratospheric intrusions. Nature communications, 6(May).
Lombardozzi, D., Levis, S., Bonan, G. and Sparks, J.P., 2012. Predicting photosynthesis and transpiration responses to ozone decoupling modeled photosynthesis and stomatal conductance. Biogeosciences, 9(8): 3113-3130.
Long, S.P., Ainsworth, E.a., Leakey, A.D.B. and Morgan, P.B., 2005. Global food insecurity. Treatment of major food crops with elevated carbon dioxide or ozone under large-scale fully open-air conditions suggests recent models may have overestimated future yields. Philosophical transactions of the Royal Society of London. Series B, Biological sciences, 360.
McGrath, J.M. et al., 2015. An analysis of ozone damage to historical maize and soybean yields in the United States. Proceedings of the National Academy of Sciences of the United States.
Mills, G. et al., 2015. Ozone impacts on vegetation in a nitrogen enriched and changing climate. Environmental Pollution.
Mills, G., Hayes, F., Wilkinson, S. and Davies, W.J., 2009. Chronic exposure to increasing background ozone impairs stomatal functioning in grassland species. Global change biology, 15(6): 1522-1533.
Mills, G. et al., 2011. New stomatal flux-based critical levels for ozone effects on vegetation. Atmospheric Environment, 45(28): 5064-5068.
Mills, G. et al., 2018a. Ozone pollution will compromise efforts to increase global wheat

production. Global change biology, 24(8): 3560-3574.
Mills, G. et al., 2018b. Closing the global ozone yield gap: Quantification and cobenefits for multistress tolerance. Global change biology, 24(10): 4869-4893.
Mitchell, M., Muftakhidinov, B. and Winchen, T., 2018. Engauge Digitizer Software.
Morgan, P.B., Ainsworth, E.A. and Long, S.P., 2003. How does elevated ozone impact soybean? A meta-analysis of photosynthesis, growth and yield. Plant, Cell and Environment, 26(8): 1317-1328.
Musselman, R., Lefohn, A., Massman, W. and Heath, R., 2006. A critical review and analysis of the use of exposure- and flux-based ozone indices for predicting vegetation effects. Atmospheric Environment, 40(10): 1869-1888.
Osborne, S.A. et al., 2016. Has the sensitivity of soybean cultivars to ozone pollution increased with time? An analysis of published dose-response data. Global change biology, 22(9): 3097-111.
Pleijel, H., Danielsson, H., Emberson, L., Ashmore, M.R. and Mills, G., 2007. Ozone risk assessment for agricultural crops in Europe Further development of stomatal flux and flux-response relationships for European wheat and potato. Atmospheric Environment, 41(14): 3022-3040.
Pleijel, H. et al., 1997. Effects of Ozone on Leaf Senescence in Spring Wheat - Possible Consequences for Grain Yield. Phyton (Austria), 37(3): 227-32.
Plöchl, M., Lyons, T., Ollerenshaw, J. and Barnes, J., 2000. Simulating ozone detoxification in the leaf apoplast through the direct reaction with ascorbate. Planta, 210(3): 454-467.
Portmann, F.T., Siebert, S. and Döll, P., 2010. MIRCA2000-Global monthly irrigated and rainfed crop areas around the year 2000: A new high-resolution data set for agricultural and hydrological modeling. Global Biogeochemical Cycles, 24(1): GB1011.
Rai, R. and Agrawal, M., 2012. Impact of Tropospheric Ozone on Crop Plants. Proceedings of the National Academy of Sciences, India Section B Biologica, 82(2): 241-257.
Rai, R., Agrawal, M. and Agrawal, S.B., 2007. Assessment of yield losses in tropical wheat using open top chambers. Atmospheric Environment, 41(40): 9543-54.
Rao, S. et al., 2016. Future air pollution in the Shared Socio-economic Pathways. Global Environmental Change.
Ray, D.K., Ramankutty, N., Mueller, N.D., West, P.C. and Foley, J.A., 2012. Recent patterns of crop yield growth and stagnation. Nature communications, 3: 1293.
Reilly, J. et al., 2007. Global economic effects of changes in crops, pasture, and forests due to changing climate, carbon dioxide, and ozone. Energy Policy, 35: 5370-5383.
Rosenzweig, C. et al., 2014. Assessing agricultural risks of climate change in the 21st century in a global gridded crop model intercomparison. Proceedings of the National Academy of Sciences of the United States of America, 111(9): 3268-73.
Schaphoff, S. et al., 2018. LPJmL4 – a dynamic global vegetation model with managed land – Part 1: Model description. Geoscientific Model Development, 11(4): 1343-1375.
Schnell, J.L. et al., 2015. Use of North American and European air quality networks to evaluate global chemistry–climate modeling of surface ozone. Atmospheric Chemistry and Physics, 15(18): 10581-10596.
Shindell, D.T., 2016. Crop yield changes induced by emissions of individual climate-altering pollutants. Earth's Future, 4.
Sitch, S., Cox, P.M., Collins, W.J. and Huntingford, C., 2007. Indirect radiative forcing of climate change through ozone effects on the land-carbon sink. Nature, 448(7155): 791-4.
Sitch, S. et al., 2003. Evaluation of ecosystem dynamics, plant geography and terrestrial carbon cycling in the LPJ dynamic global vegetation model. Global Change Biolgoy,

9(2): 161-185.
Sofen, E.D. et al., 2016. Gridded global surface ozone metrics for atmospheric chemistry model evaluation. Earth System Science Data, 8(1): 41-59.
Solazzo, E. et al., 2017. Evaluation and error apportionment of an ensemble of atmospheric chemistry transport modeling systems: multivariable temporal and spatial breakdown. Atmospheric Chemistry and Physics, 17(4): 3001-3054.
Stevenson, D.S. et al., 2006. Multimodel ensemble simulations of present-day and near-future tropospheric ozone. Journal of Geophysical Research, 111(8).
Stjern, C.W. et al., 2016. Global and regional radiative forcing from 20 % reductions in BC, OC and SO4 – an HTAP2 multi-model study. Atmospheric Chemistry and Physics, 16(21): 13579-13599.
Tai, A.P.K., Martin, M.V. and Heald, C.L., 2014. Threat to future global food security from climate change and ozone air pollution. Nature Climate Change(July).
The Royal Society, 2008. Ground-level ozone in the 21st century future trends, impacts and policy implications.
Tuzet, A., Perrier, A., Loubet, B. and Cellier, P., 2011. Modelling ozone deposition fluxes: The relative roles of deposition and detoxification processes. Agricultural and Forest Meteorology, 151(4): 480-492.
Van Dingenen, R. et al., 2009. The global impact of ozone on agricultural crop yields under current and future air quality legislation. Atmospheric Environment, 43(3): 604-618.
Waha, K., van Bussel, L.G.J., Müller, C. and Bondeau, A., 2012. Climate-driven simulation of global crop sowing dates. Global Ecology and Biogeography, 21(2): 247-259.
Warszawski, L. et al., 2014. The Inter-Sectoral Impact Model Intercomparison Project (ISI-MIP): project framework. Proceedings of the National Academy of Sciences of the United States of America, 111(9): 3228-32.
Weedon, G.P. et al., 2014. The WFDEI meteorological forcing data set: WATCH Forcing Data methodology applied to ERA-Interim reanalysis data. Water Resources Research, 50: 7505-7514.
Wilkinson, S. and Davies, W.J., 2010. Drought, ozone, ABA and ethylene new insights from cell to plant to community. Plant, Cell and Environment, 33: 510-25.
Wilkinson, S., Mills, G., Illidge, R. and Davies, W.J., 2012. How is ozone pollution reducing our food supply. Journal of experimental botany, 63(2): 527-36.
Yin, X. and Struik, P.C., 2009. C3 and C4 photosynthesis models: An overview from the perspective of crop modelling. NJAS - Wageningen Journal of Life Sciences, 57(1): 27-38.
Zampieri, M. et al., 2018. Surface Freshwater Limitation Explains Worst Rice Production Anomaly in India in 2002. Remote Sensing, 10(2): 244.
Zhu, X. et al., 2011. Effects of elevated ozone concentration on yield of four Chinese cultivars of winter wheat under fully open-air field conditions. Global change biology, 17(8): 2697-2706.